STAT3 ameliorates cognitive deficits by positively regulating the expression of NMDARs in a mouse model of FTDP-17

Gong-Ping Liu (liugp111@mail.hust.edu.cn)
Huazhong University of Science and Technology Tongji Medical College https://orcid.org/0000-0001-8501-998X

Xiao-Yue Hong
Huazhong University of Science and Technology Tongji Medical College

Hua-Li Wan
Huazhong University of Science and Technology Tongji Medical College

Ting Li
Huazhong University of Science and Technology Tongji Medical College

Bing-Ge Zhang
Huazhong University of Science and Technology Tongji Medical College

Xiao-Guang Li
Huazhong University of Science and Technology Tongji Medical College

Xin Wang
Huazhong University of Science and Technology Tongji Medical College

Xiao Li
Huazhong University of Science and Technology Tongji Medical College

Qian Liu
Huazhong University of Science and Technology Tongji Medical College

Chong-Yang Chen
Huazhong University of Science and Technology Tongji Medical College

Ying Yang
Huazhong University of Science and Technology Tongji Medical College

Qun Wang
Huazhong University of Science and Technology Tongji Medical College

Shu-Peng Li
Peking University

Hao Yu
Shenzhen Polytechnic

Jian-Zhi Wang
Huazhong University of Science and Technology Tongji Medical College

Xi-Fei Yang
Shanxi Center for Disease Control and Prevention

Research article

Keywords: P301L-hTau, STAT3, synapse, N-methyl-D-aspartate receptors, memory

Posted Date: May 7th, 2020

DOI: https://doi.org/10.21203/rs.3.rs-25793/v1

Abstract

Background In tauopathies, the degree of neurodegeneration and memory impairment positively strongly correlates with the amount of abnormal tau aggregates. Recently, we found that human wild-type tau accumulation activated Signal Transduction and Activator of Transcription-1 (STAT1) to inhibit the transcription of genes coding for synaptic N-methyl-D-aspartate receptors (NMDARs). STAT3 has similar specific DNA binding element GAS as STAT1, however, the role of STAT3 in cognitive deficits induced by tau accumulation has not reported until now.

Methods The activity of the transcription factor was analyzed by luciferase reporter assay or electrophoresis mobility shift assay. AAV virus (AAV-Cre, AAV-P301L, AAV-STAT3 or AAV-K410/3R-STAT1) was infused stereotaxically into the hippocampal CA3 regions of $STAT3^{flox/flox}$ or C57 mice. The spatial learning and memory of the animals were assessed by Morris water maze, the contextual fear conditioning and new object recognition test. The synaptic plasticity was measured by electrophysiological recording and the spine density was detected by Golgi staining. RT-PCR and Western blotting were used to detect the mRNA and protein levels.

Results We found that P301L-hTau accumulation acetylated STAT1 at lysine 410 and 413 sites to bind with STAT3 in the cytoplasm which inhibited the nuclear translocation and inactivated STAT3, though phosphorylation of STAT3 at Tyr705, which leads to STAT3 nuclear translocation and DNA binding, increased. Knockdown of STAT3 by AAV-Cre in $STAT3^{flox/flox}$ mice mimicked P301L-hTau-induced suppression of NMDARs expression, synaptic and memory impairments. Overexpressing STAT3 rescued P301L-hTau-induced synaptic and cognitive deficits by increasing NMDARs expression. Further study revealed that STAT3 positively regulated NMDARs transcription through direct binding to the specific GAS element of NMDAR1, NMDAR2A and NMDAR2B promoters.

Conclusion These findings indicate that accumulated P301L-hTau impairs synaptic plasticity by inactivating STAT3 to suppress NMDARs expression, thereby revealing a novel mechanism for P301L-hTau-associated synapse and cognition deficits.

Background

Neurofibrillary tangles composed of the misfolded hyperphosphorylated Tau, are involved in more than 20 kinds of neurodegenerative diseases, including Alzheimer's disease (AD), frontotemporal dementia (FTDP-17), progressive supranuclear palsy, and so on, which collectively referred to as ‘tauopathies’ [1–3]. Braak staging is used to describe the stages and location of neurofibrillary tangles in AD [4], and the degree of neurodegeneration and memory impairment are strongly correlated with the amount of abnormal tau-aggregates in the brain [5]. Additional, the total level of tau protein in cerebrospinal fluid is inversely related to scored memory [5, 6].

Animal studies strongly support clinical evidence that tau plays a key role in learning and memory disorders. For example, transgenic mice expressing the most common FTDP-17 mutation (P301L)

develop neurofibrillary tangles and behavioral deficits in an age- and gene-dose-dependent manner [7]. Overexpression of full length human tau40 (htau) also triggers pathological changes and memory impairment in the brain of transgenic mice [8, 9], while inhibition of tau expression or immunotherapy against pathological tau improves memory impairment and reduces neuronal loss in htau transgenic mice [10, 11].

Tau protein is essential for the neurotoxic effects of Aβ, another key pathological component of AD. Knocking-out tau protein or truncated tau (Deltatau) can improve memory deficits found in Aβ-forming APP23 transgenic mice overexpressing human APP with the Swedish double mutation [12], and reducing endogenous tau can improve behavioral disorders of transgenic mice overexpressing human APP, but does not alter Aβ levels [13]. Phosphorylation of tau at specific sites can also inhibit Aβ neurotoxicity [14].

Tau is a key microtubule-associated protein that promotes the assembly and maintains the stability of microtubules in nerve cells required for axonal transport and maintenance of neuronal integrity [15, 16]. Tau hyperphosphorylation results in the dissociation of microtubules and disruption of molecular axonal transport. Recent studies show that phosphorylated tau supports cell viability by antagonizing apoptotic factors [17–19]. Tau hyperphosphorylation occurs not only in axons but also in cell bodies and dendrites [12].

We have reported elsewhere that abnormal tau protein accumulates in cells in disorders of mitochondrial dynamics, mitophagy deficits, and mitochondria dysfunction associated with increasing mitochondrial membrane potential [20, 21]. In primary culture neurons, accumulated tau was found to activate calcineurin to dephosphorylate CREB and calcium/calmodulin-dependent protein kinase IV (CaMKIV), which thereby perturbed intracellular calcium signaling [22]. Tau accumulation also repressed autophagy by disrupting IST1-regulated ESCRT-III complex formation [23]. These studies partially disclose the mechanisms underlying the toxic effects of tau. However, the molecular mechanisms underlying hTau-induced synapse impairment are not fully understood.

Recently, we found that accumulating htau increases JAK2 activity to phosphorylate STAT1 (signal transducer and activator of transcription-1), which decreased *N*-methyl-D-aspartate receptor (NMDAR) expression by directly binding to the specific GAS elements in NMDARs promoters (GluN1, GluN2A, GluN2B) and thereby inhibiting their transcription [24]. STAT1 and signal transduction and activator of transcription-3 (STAT3) both belonging to STAT protein family, have similar specific DNA binding element GAS and are both reported to involve in cognition [25–32]. In the present study, we found that overexpressing P301L-hTau (P301L), that the mutation can directly result in neurodegeneration [33], inhibited STAT3 to transport from the cytoplasm into the nucleus to inactivate STAT3 through increasing the interaction of acetylated STAT1 and STAT3 in the cytoplasmic fraction. Overexpressing STAT3 attenuated the P301L-induced synaptic and cognitive deficits. We also found that STAT3 can directly bind the specific GAS element in GluN1, GluN2A or GluN2B promoter and thus activate expression of NMDARs, which reveals a novel mechanism underlying Tau-induced synapse impairment of cognitive deficits.

Methods

Antibodies and reagents

The antibodies used in the present study are listed in the Additional file 1: Table S1. TG-101348 (special JAK2 inhibitor, from MCE), JAK2 siRNA (sc-39099, from Santa Cruz Biotechnology), SP600125 (the inhibitor of JNK1, from Santa Cruz) and FR180204 (the inhibitor of ERK1, from Santa Cruz) were purchased. PcDNA3.0 vector coded wild type STAT1 (WT-STAT1) plasmid was the gift of Dr. Xiao-Yuan Li (Institute of Biomedical Sciences, Academia Sinica, Taiwan), and PcDNA3.0 vector coded wild type STAT3 (WT-STAT3) plasmid was purchased from Shangdong Vigene Bioscience Biotechnology, co., LTD. EGFP-N1 vector coded mutant full-length human tau (P301L-hTau) plasmid, WT-STAT1 plasmid was mutated to pseudoacetylated STAT1 plasmids (single or double lysine sites (410, 413) mutated to glutamine, K410Q-, K413Q-, K410/3Q-STAT1) or unacetylated STAT1 plasmids (single or double lysine site (410, 413) mutated to arginine, K410R-, K413R-, K410/3R-STAT1) coded into RFP-N1 vector by Shanghai Baicheng Biotechnology, co., LTD.

Animals

Male C57 mice were purchased from the Animal Center of Tongji Medical College, Huazhong University of Science and Technology. $STAT3^{flox/flox}$ mice (B6; 129S-STAT3tm1Mam/Mmjax) and Tg4510 mice (FVB-Fgf14Tg(tetO-MAPT*P301L)4510Kha/JlwsJ) were purchased from Jackson Laboratory. All mice were kept at 22 ± 2 ºC on 12 h light-dark cycles with ad libitum access to food and water. All animal experiments were performed according to the 'Policies on the Use of Animals and Humans in Neuroscience Research' revised and approved by the Society for Neuroscience (USA) in 1995, and the Guidelines for the Care and Use of Laboratory Animals of the Ministry of Science and Technology of the People's Republic of China. The Institutional Animal Care and Use Committee at Tongji Medical College, Huazhong University of Science and Technology approved the study protocol.

Stereotaxic brain injection

Adeno-associated virus coded for human mutant full-length P301L-hTau (AAV-P301L) with the N-terminal fused with enhanced green fluorescent protein (eGFP) and the control AAV-eGFP, AAV-STAT3, AAV-K410/3R-STAT1 virus were purchased from OBio Biologic Technology Co., Ltd. AAV-cre was purchased from Shanghai Genechem Co.,Ltd. The titer of AAV-P301L was 1.3×10^{13} v.g./ml, that of AAV-STAT3 virus was 1.2×10^{13} v.g./ml, and the titer for AAV-K410/3R-STAT1 virus was 1.1×10^{13} v.g./ml. The titer of AAV-Cre or the control virus was 7.9×10^{12} v.g./ml. All AAV viruses were driven by CMV-promoter. The *in vivo* overexpression efficiency was measured by immunohistochemical staining and Western blotting 1 month later after injection of the virus into the hippocampal CA3 region of mice. After positioned in a stereotaxic instrument, 3 month-old C57 or $STAT3^{flox/flox}$ mice were bilaterally injected the virus into the hippocampal CA3 region (AP ±2.0, ML -1.5, DV -2.0) at a rate of 0.10 μl/min. The needle syringe was left in place for ~3

min before being withdrawn. The injection did not significantly change the normal activity or increase the death rate of the mice compared with the non-injected controls.

Behavioral tests

~1 month after brain infusion of the virus, Morris water maze (MWM) test was used to assess spatial learning and memory [34]. For spatial learning, mice were trained to find a hidden platform in the water maze for 6 consecutive days, 4 trials per day with a 30 s interval from 14:00 to 20:00 pm. On each trial, an operator let the animal face the wall of the pool and started from one of the four quadrants. When the animal climbed on the platform, the trial ended. If the mice did not locate the platform within 60 s, operators guided them to the platform and stayed for 30 s. The spatial memory was tested 24 h after the last training. The longer a mouse stayed in the quadrant where the platform previously located, the higher the score for spatial memory. The swimming path and the latency to find the platform or times passing through the previous platform-located quadrant (during test phase) were recorded by a video camera. The camera was fixed to the ceiling, 1.5 m from the water surface, and connected to a digital-tracking device, which attached to an IBM computer.

The contextual fear conditioning test was performed according to our previously established procedure [35]. Briefly, prior to experimentation, in order to adapt to the environment, the mouse was kept in the cage for 3 min. The animal then received training via 3 min unsignaled foot-shocks (one shock at the 1st min, three shocks at the 2nd min and 8 shocks at the 3rd min; 0.5 mA, 2-sec duration, and 1 min apart). Long-term memory (LTM) was tested respectively 24 h post-training by placing the animal back into the conditioning chamber for 3 min and measuring the freezing time.

The new object recognition test was performed according to a published procedure [36]. A 5-min habituation without objects was conducted. After one hour, an object familiarization phase with two of Object A for 5 min was conducted. A further 5-min testing period with one of Object A and Object B, which were randomly assigned as A and B, was conducted after one hour later. A blinded investigator scored object recognition times. The novel object recognition ratio was calculated as: [(time novel object)/(time novel object +time familiar object)]. Object exploration was defined as active investigation of an object within ~2 cm or less of its nose.

Electrophysiological analysis

A Leica VT1000S vibratome (Milton Keynes, UK) was used to cut horizontal brain slices (400 μm) containing the dorsal hippocampus at 4 º C in artificial cerebrospinal fluid (aCSF), which consisted of: 126 mM NaCl, 3 mM KCl, 1.25 mM NaH_2PO_4, 24 mM $NaHCO_3$, 2 mM $MgSO_4$, 2 mM $CaCl_2$ and 10 mM glucose (pH 7.4; 305 mOsm), and saturated with carbogen (95% O_2 and 5% CO_2). Immediately after slicing, sections were transferred and maintained in an interface chamber continuously perfused with aCSF, and the slices were equilibrated at least for 30 min prior to recording at room temperature.

For extracellular recordings, slices were placed in the interface recording chamber at 32 º C and the perfusion rate was normally 3 ml/min, while maintaining a thin film of aCSF covering the slice to make sure applied substances could diffuse into the area recorded. Field potentials were amplified with Neurolog AC-coupled NL 104 preamplifiers (Digitimer Ltd, Welwyn, UK). The excitatory postsynaptic potential (fEPSP) was recorded by a 0.1-MΩ tungsten monopolar electrode from the dendritic layer of the stratum radiatum of the CA3 field following electrical stimulation of the mossy-fiber pathway. The electrical pulses were delivered using a bipolar platinum/iridium electrode (25 mm wire-diameter, at an inter-wire distance of 100 mm, World Precision Instruments, USA). The fEPSP was quantified by 30 % of the maximum slope of its rising phase. We used theta-burst stimulation (TBS), which consisted of 4 pulses at 100 Hz, repeated 3 times with a 200-ms interval, to induct long-term potentiation (LTP). LTP magnitude was expressed as the mean percentage of baseline fEPSP initial slope [37, 38].

Cell culture

HEK293 (human embryonic kidney293) were cultured in Dulbecco's Modified Eagle's medium (DMEM), supplemented with fetal bovine serum (10%, v/v) and penicillin/streptomycin (1%), in a humidified atmosphere containing 5% CO_2 at 37 ºC. The cells grew in plates for 24 h, and then the indicated plasmid(s) were transfected into the cells using Lipofectamine2000 according to the instructions of manufacturers.

For primary neuron cultures, 18-day embryonic (E18) hippocampus of rat was seeded on 6-well plates at 30,000-40,000 cells per well, which coated with Poly-D-Lysine/Laminin (Bioscience) in neurobasal medium (Invitrogen) supplemented with B27 (2%)/ glutamine (0.5 mM) / glutamate (25 mM). Half the culture medium was changed every 2 days with neurobasal medium supplemented with B27 (2%) and glutamine (0.5 mM). All cultures were kept at 37 º C in a humidified 5% CO_2-containing atmosphere. After cultured for 7 to 17 div, more than 90% of the cells were neurons, which was verified by positive staining for the neuronal specific marker MAP2 (dendritic marker, Millipore).

Preparation of nuclear fractionation

According to instructions of the manufacturer, the nuclear extracts were prepared using the nuclear extraction kit (Signosis, Inc., Sunnyvale, CA, USA). Briefly, Buffer I working reagent was added to the culture dish and rocked at 200 rpm on a shaking platform at 4 º C for 10 min. The HEK293 cells were collected and centrifuged at 12,000 rpm at 4 ºC for 5 min. The supernatant was discarded, and the pellets were re-suspended by adding Buffer II working reagent. For tissues, the hippocampal CA3 areas (location of viral infected) were rapidly cut into small pieces, added Buffer I working reagent, and homogenized at 4 ºC until a single cell suspension was observed microscopically. After spinning at 500 g at 4 ºC for 5 min, and the supernatant was removed, the cell pellets were re-suspended in Buffer I working reagent, and the preparation rocked at 200 rpm on a shaking platform at 4 ºC for 10 min. The cells were then centrifuged at 10,000 rpm at 4 ºC for 5 min, and the pellets were re-suspended by adding Buffer II working reagents. Lastly, the cell lysate was shaken at 200 rpm on a platform at 4 ºC for two hours. After

centrifugation at 12,000 rpm at 4 ºC for 5 min, the supernatant (nuclear extract) was collected and stored at -80 ºC until use.

Preparation of insoluble tau

Insoluble tau aggregates were isolated from the virus infected-hippocampal tissue by a modification of a published procedure [23]. Brain tissues were homogenized in lysis buffer (in mM): Tris-HCl 10, NaCl 150, NaF 20, Na_3VO_4 1, EGTA 2, Triton X-100 0.5%, and SDS 0.1% with protease inhibitor mixture and centrifuged at 13,000 × g for 20 min. The resulting supernatant was designated as the soluble tau fraction. The pellet was resuspended in 1% SDS buffer with 10 times ultrasonication and designated as insoluble aggregated tau.

Western blotting

10% sodium dodecyl sulfate-polyacrylamide gel electrophoresis (SDS-PAGE) was used to separate equal amounts of protein, and the separated proteins were transferred onto nitrocellulose membranes. For analysis of STAT3 dimerization, cell lysates were incubated with 1 mM DSS, blocked with 0.5 mM NH_4OH for 20 min, and then, used for Western blotting [39]. The membranes were blocked in non-fat milk (5%) at 20 ºC for 1 h and then incubated with primary antibody (Additional file 1: Table S1) at 4 ºC overnight. Blots were then incubated with IRDye 800CW-conjugated affinity-purified anti-mouse IgG (Rockland) or IRDye 800CW anti-rabbit IgG secondary antibody (Rockland) at 20 ºC for 1 h. Odyssey Infrared Imaging System (Licor Biosciences, Lincoln, NE, USA) was used to visualize immunoreactive bands.

Reverse transcription and real-time quantitative PCR

According to manufacturer's instruction (TaKaRa, Dalian, China), reverse transcription and real-time quantitative PCR were carried out. The PCR system contained $MgCl_2$ (3 mM), forward and reverse primers (0.5 μM), SYBR Green PCR master mixes (2 μl) and cDNA (2 μl), and the standards for each gene. A Rotor Gene 300 Real-time Cycler (Corbett Research, Sydney, Australia) was used to assay the samples. Glyceraldehyde-3-phosphate dehydrogenase (GAPDH), the housekeeping gene which was not changed by the treatments, was used to normalize the expression level of the interest gene. PCR primers employed in the present study are as follow: Mmu-GluA1 forward and reverse primers, 5'-CAATGACCGCTATGAGGG-3' and 5'- AAGGACTGAAACGGCTGA-3'; mmu-GluA2 forward and reverse primers, 5'-GTGTCGCCCATCGAAAGTG-3' and 5'-AGTAGGCATACTTCCCTTTGGAT-3'; mmu-synapsin1 (Syn1) forward and reverse primers, 5'- AGGACGAGGTGAAAGC-3' and 5'-TCAGTCGGAGAAGAGG-3'; mmu-synaptotagmin1 (Syt1) forward and reverse primers, 5'- CCATAGCCATAGTTGC-3' and 5'-GTTTCAGCATCGTCAT-3'; mmu-GluN1 forward and reverse primers, 5'- GTCCACCAGACTAAAGA-3' and 5'-TCCCATCATTCCGT-3'; mmu-GluN2A forward and reverse primers, 5'- CTTTTGAGGACGCC-3' and 5'-AAATGAGACCCGATG-3'; mmu-GluN2B forward and reverse primers, 5'- GGCTGACTGGCTACG-3' and 5'-CTTGGGCTCAGGGAT-3'; mmu-GAPDH forward primer 5'-GGAGCGAGATCCCTCCAAAAT-3' and reverse primer 5'-GGCTGTTGTCATACTTCTCATGG-3'.

Electrophoresis mobility shift assay (EMSA)

The non-radioactive EMSA-STAT3 Kit was purchased from Signosis (Sunnyvale, CA, USA). EMSA was performed according the instruction of the manufacturer. Briefly, a biotinized oligonucleotide probe which containing a STAT3 binding site, were incubated with the samples, and then, the samples were separated on a non-denaturing polyacrylamide gel and transferred to nylon membranes. UV crosslinking was used to immobilize the transferred oligonucleotides. In order to detect the oligonucleotides, Streptavidin-HRP was added to the membrane, and the blots were developed by ECL according to the instructions of manufacturers. Excess amounts of unlabeled cold probe which containing STAT3 binding site, was used to perform a competition experiment.

Luciferase reporter assay

Activity of the transcription factors (TFs) was analyzed with the specific luciferase reporter vector pSTAT3-Luc (Signosis). This vector contains a cis-element (DNA binding sequence), a minimal promoter, and a firefly luciferase gene. The activated transcription factors binds to the cis-element and transactivates expression of the luciferase gene correlating with the measured luciferase enzyme activity. Therefore, the luciferase activity in this assay represents activation of the transcription factor. Briefly, HEK293 cells were transfected with P301L-hTau plasmid or its empty vector control in combination with pSTAT3-Luc reporter construct and pRL-TK for 48 h. Then the cells were washed and lysed in 100 μl of the 1×CCLR (Promega). Luciferase activity was measured according to the manufacturer's instruction (Promega). The activity of TF (i.e. firefly luciferase) was normalized to transfection efficiency by using Renilla luciferase activity (pRL-TK).

To generate luciferase reporter plasmids of GluN1, GluN2A or GluN2B promoter, after copied from the mouse genomic DNA, PCR fragments were subcloned into pGL3 basic luciferase expression vector (Promega, Madison, WI) between the BglII and NcoI sites. The GeneTailor system (Invitrogen) was used to introduce mutation of the pGL3-GluN1/GluN2A/GluN2B luciferase plasmid. Luciferase reporter plasmids were transfected into HEK293 cells by Lipofectamine Plus (Invitrogen) according to the manufacturer's instructions. To assay the luciferase activity, pGL3-construct, P301L-hTau and pRL-TK plasmid were co-transfected into HEK293 cells, after the cells were seeded into 24-well plates one day prior to transfection. 24 h later, cells were harvested and lysed with Passive Lysis Buffer (100 μl). 20 μl cell extracts were used for luciferase activity assay by a Lumat LB9507 luminometer (Berthold) and the Dual Luciferase Reporter (DLR) assay system (Promega).

Chromatin immunoprecipitation (ChIP) assay

The DNA and protein were cross-linked with formaldehyde (1%) for 10 min, and washed 3 times and scraped into cold PBS with protease inhibitors. After centrifugation, the cell pellet was re-suspended in buffer (in mM): 20 HEPES, pH 7.9, 420 NaCl, 1.5 $MgCl_2$, and 0.2 EDTA, with 25 % glycerol and protease inhibitors, incubated for 20 min on ice, and centrifuged. The pellet (nucleus) was re-suspended in breaking buffer (in mM): 50 Tris-HCl, pH 8.0, 1 EDTA, 150 NaCl with 1 % SDS, 2 % Triton X-100 and

protease inhibitors, and sonicated for 5~10 s, and Triton buffer (in mM): 50 Tris-HCl, pH 8.0, 1 EDTA, 150 NaCl, with 0.1% Triton X-100 was added. An aliquot was reserved as the input, and the remainder was divided to immunoprecipitate with control mouse IgG (Millipore,) or STAT3 (Abcam) antibody and incubated with protein G beads. After washed 3 times in Triton buffer, the samples were added with SDS buffer consisted of 62.5 mM Tris-HCl, pH 6.8, 200 mM NaCl, 2 % SDS, 10 mM DTT, 2 μl of proteinase K (40 mg/ml), and then, samples were vortexed. To reverse cross-linking, samples were incubated at 65 ºC overnight. After isolated using phenol/chloroform extraction, DAN was re-suspended in distilled H_2O. Primers used for ChIP PCR were as following: GluN1 forward and reverse primer, 5'-TAGCATTGGCATTGACCC-3', 5'-GCTGGTGCGGTGATGTGA-3'; GluN2A forward and reverse primer, 5'-TCGGCTTGGACTGATACGTG-3', 5'- AGGATAGACTGCCCCTGCAC-3'; GluN2B forward and reverse primer, 5'- TCTCCACCGTGCTGATGT-3', 5'-CTCTCCGAGTCTACCTGTTC-3'. PCR products were analyzed by 2% agarose gel electrophoresis.

Immunohistochemistry

In brief, mice were terminated using chloral hydrate (1 g/kg) and perfused through aorta with physiological saline (100 ml) followed by phosphate buffer containing 4 % paraformaldehyde (400 ml). After removed and postfixed in perfusate overnight, brains were cut into sections (30 μm) using a vibratome (Leica, Nussloch, Germany; S100, TPI), and then, sections were collected consecutively in PBS for immunohistochemistry. Free floating sections or FTDP-17 brain sections were blocked with 0.3% H_2O_2 in absolute ethanol for 30 min at room temperature, and incubated with bovine serum albumin (BSA) for another 30 min to block nonspecific sites. Primary antibodies were used to incubate with sections at 4 ºC overnight. Immunoreaction was developed and visualized with diaminobenzidine (brown color) by Histostain TM-SP kits. FTDP-17 brain sections were counterstained with hematoxylin, and mouse or human sections dehydrated through a graded ethanol series, mounted on glass slides, and sealed with glass coverslips. For each primary antibody, 3-5 consecutive sections from each brain were used. A microscope (Olympus BX60, Tokyo, Japan) was used to observe the images.

The human brain tissues used in the present study were provided by Dr. K Ye of the Emory University School of Medicine, USA (Additional file 1: Table S2). The study was approved by the Biospecimen Committee. Informed consent was obtained from the subjects.

Statistical analysis

All data were collected and analyzed in a blinded manner. Data were expressed as mean ± SD or mean ± SEM. Statistical analysis was performed using Mann-Whitney test (two-group comparison), one-way ANOVA or two-way repeated measures ANOVA followed by Bonferroni's post hoc test with SPSS 12.0 statistical software (SPSS Inc. Chicago, IL, USA). A p-value of < 0.05 was considered as statistical significance in all experiments.

Results

Intracellular P301L-hTau accumulation inactivates STAT3 despite the level of phosphorylated STAT3 increases

In our previous study, we found that the accumulated htau increased STAT1 activity, while the activity of HNF1, HOX4C, PLAG1, SMUC, VDR, SF-1 and PIT1 decreased remarkably [24]. STAT3 and STAT1 belong to the STAT protein family, and both are reported to be involved in cognitive functions [25-32]. Herein, we investigated the effects of P301L-hTau accumulation on STAT3 activity, and if so, the role of STAT3 in P301L-hTau-induced cognitive deficits and the underlying molecular mechanisms.

We demonstrated that overexpressing P301L-hTau markedly increased the phosphorylation of STAT3 at Tyr705 (pY705) in cell extracts (Fig. 1a and c), but decreased total STAT3 and the activity-dependent phosphorylation of STAT3 at Ser727 (pS727) in the nuclear fraction (Fig. 1b and d) with a decreased nuclear translocation (Fig. 1e) and dimerization (Fig. 1f) of STAT3 measured by Western blotting and immunofluorescence imaging. Inactivation of STAT3 by overexpressing P301L-hTau was also confirmed by TF luciferase assay (Fig. 1g). By EMSA, using an oligonucleotide probe containing STAT3 binding site, we found that P301L-hTau accumulation decreased binding of STAT3 to DNA, and this association was disrupted by using cold probe (Fig. 1h). To verify the specificity of STAT3 inactivation, we studied the effects of TDP-43 and alpha-synuclein on STAT3 in HEK293 cells. The results showed that overexpression of TDP-43 or α-synuclein did not significantly alter the total and nuclear levels of STAT3 and p-STAT3 (Additional file 1: Figure S1), indicating that STAT3 inactivation may be specific for P301L-hTau. These *in vitro* data indicated that intracellular P301L-hTau accumulation inhibited STAT3 activity.

To test the in vivo effects of P301L-hTau accumulation on STAT3, we first injected stereotaxically AAV-P301L-hTau into the mouse hippocampi and detected the alterations of STAT3 and pY-STAT3 after 1 month. The virus mainly infected neurons rather than microglia or astrocytes (Additional file 1: Figure S2). Expression of P301L-hTau was confirmed by Western blotting (Fig. 1i), and accumulation of misfolded tau was shown by Thioflavin-S staining (Additional file 1: Figure S3). Overexpression of P301L-hTau significantly increased total pY705-STAT3 in hippocampal extracts but decreased total and pS727-STAT3 in the nuclear fraction (Fig. 1i to j). A decreased nuclear translocation of STAT3 was also measured immunofluorescence imaging (Fig. 1k). In the cortex of FTDP patients which had a P301L mutation of Tau, STAT3 in the nucleus was also significantly decreased (Fig. 1l). These data provide the *in vivo* and human evidence for the role of P301L-hTau accumulation in inhibiting STAT3 activity.

Intracellular P301L-hTau accumulation increases the interaction of STAT1 and STAT3 in the cytoplasm by acetylation of STAT1

Phosphorylation of STAT3 at tyrosine 705 (pY-STAT3) is reported to lead to STAT3 nuclear translocation and DNA binding [40, 41]; however, in the present study, we found that P301L decreased the level of STAT3 in the nuclear fraction while pY-STAT3 in the total lysates increased. To probe for the cause, Co-IP assay was used to detect the interaction of STAT3 and STAT1. This showed that intracellular P301L

accumulation increased the interaction of STAT1 and STAT3 in both total lysates and the cytoplasm fraction but decreased the interaction in the nuclear fraction (Fig. 2a to b).

Previous studies reported that acetylation of STAT1 enhanced the binding of STAT1 with NF-κB p65 to inhibit NF-κB p65 nucleation [42]. To verify whether acetylation of STAT1 inhibited STAT3 nucleation in the same way, we detected the acetylation of STAT1 by mass spectrometry (Fig. 2c). We obtained a lysine acetylation signal from the peptide fragment HLQLKEQKNAGTR, among which two lysine residues corresponded to lysine 410 (K410) and lysine 413 (K413) of STAT1, respectively. Intracellular P301L-hTau accumulation increased the acetylation of STAT1 in both cell lysates and the cytoplasm but decreased the acetylated level in the nuclear fraction by IP assay (Fig. 2d).

To investigate the mechanisms underlying the increase of acetylated STAT1 induced by P301L-hTau, we measured CBP, p300 and HDAC2, which are involved in protein acetylation modification [42-44]. However, P301L-hTau overexpression did not change the protein level of p300 and HDAC2 but decreased CBP in cell lysates (Fig. 2e to f), which together exclude involvement of CBP, p300 and HDAC2 in acetylating STAT1. Tau itself acts as acetylase [45]. *In vitro* assay showed that the recombinant protein P301L-hTau increased acetylated level of STAT1 (Fig. 2g). We also found that overexpressing P301L increased the binding with STAT1 in HEK293 cells (Fig. 2h). The repeat domain of tau protein, namely K18, mediates the acetyl transferase action of tau [45]. We transfected the K18-deleted P301L (K18(-)) plasmid into HEK293 cells and found that K18(-) did not affect the acetylated STAT1 level and the interaction of STAT1 and STAT3 in total, cytoplasm and nuclear fraction compared with the control (Fig. 2i, additional file 1: Figure S4). Overexpressing K18(-) also did not change the distribution of STAT3 protein in the nuclear fraction (Fig. 2j to k). The above results indicated that P301L-hTau accumulation inhibited STAT3 transport into the nucleus by increasing the interaction of STAT3 with STAT1 in the cytoplasm via acetylation of STAT1.

STAT1 acetylation inhibited STAT3 nuclear translocation

To further verify the effect of STAT1 acetylation on STAT3 nucleation, we used pseudoacetylated (K410Q, K413Q and K410/413Q) or unacetylated (K410R, K413R, K410/413R) mutant STAT1 plasmids at single or double sites. Protein in the total cell lysis and nuclear fractions were extracted and detected by Western blotting, respectively. Only K410/413Q not K401Q or K413Q-STAT1 significantly reduced the level of STAT3 in the nuclear fraction, and the nuclear STAT3 level showed a decline with overexpression of pseudoacetylated mutant of STAT1 in single site (K410Q or K413Q) (Fig. 3a to c). Nonacetylated mutant STAT1 (K410R, K413R or K410/413R) had no effect on the STAT3 level in the nuclear fraction (Fig. 3d to f). Neither pseudoacetylated nor unacetylated STAT1 mutant changed the STAT3 level in the total extract (Fig. 3a, c, d and f). The non-acetylated STAT1 mutant at the double site (K410/413R) ameliorated P301L-induced reduction of STAT3 level in the nuclear fraction (Fig. 3g to i). We also found by luciferase assay that overexpression of K410/413Q-STAT1 plasmid decreased STAT3 activity, and K410/413R-STAT1 attenuated the P301L-induced reduced STAT3 activity (Fig. 3j to l).

STAT3 knockdown by AAV-Cre induces synaptic plasticity and cognitive impairments in STAT3$^{flox/flox}$ mice

To investigate the role of STAT3 in learning and memory function [30-32], we first infused AAV-Cre into the hippocampal CA3 zone of 2-month-old STAT3$^{flox/flox}$ mice to knockdown STAT3 and then assayed cognitive ability one month later (Fig. 4). The efficiency of AAV-Cre in downregulating STAT3 was confirmed by Western blotting (Fig. 4a) and immunohistochemistry (Fig. 4b). By MWM test, we observed that STAT3 knockdown efficiently induced learning impairments shown by the increase of escape latencies at days 2, 3, 5 and 6 during the 6-day training period (Fig. 4c). In the memory test (measured at day 7 by removal of the escape platform), STAT3 knockdown mice showed a longer average latency to reach the previous target quadrant (Fig. 4d); relative to control mice, they crossed the platform quadrant fewer times (Fig. 4e) and stayed for a shorter period in the platform quadrant (Fig. 4f). No significant difference in swimming speed was seen between the two groups (Fig. 4g), which excluded motor deficits. By the new object recognition test, STAT3 knockdown was associated with deficiency in recognizing a novel object (Fig. 4h). By contextual fear conditioning test, we also observed that STAT3 knockdown impaired long-term memory, as shown by a decreased freezing time during the memory test (Fig. 4j). The fEPSP slope and the density of dendrite spines were also reduced by STAT3 knockdown (Fig. 4k to n). These data demonstrate that downregulating STAT3 in the hippocampus can efficiently induce learning and memory impairments.

STAT3 overexpression ameliorates P301L-hTau-induced synaptic plasticity and memory deficits

To further certify the role of STAT3 in P301L-hTau-induced cognitive deficits, we co-injected AAV-P301L-hTau and AAV-STAT3 bilaterally into the hippocampal CA3 regions of 2-month-old C57 mice for 1 month. Overexpression of STAT3 was proved by Western blotting (Fig. 5a) and immunofluoresence (Fig. 5b). P301L-hTau impaired learning and memory abilities as detected by the MWM test (Fig. 5c to h), new novel object recognition test (Fig. 5i) and the conditional fear conditioning test (Fig. 5j to k), with reduction of fEPSP slope and dendrite spine density (Fig. 5l to o). Overexpression of STAT3 attenuated P301L-hTau-induced cognition and dendritic plasticity impairments (Fig. 5). These data show that STAT3 plays a critical role in P301L-hTau-induced dendritic plasticity and cognitive deficits.

To explore whether STAT3 overexpression affects tau phosphorylation and aggregation, we extracted soluble and insoluble tau from the hippocampal CA3 and detected protein levels by Western blotting. Reduction of phosphorylated tau at Ser214, Thr231, Ser396 and Ser404 in the insoluble fraction was shown by overexpressing STAT3 (Additional file 1: Figure S5). These data suggested that overexpressing STAT3 attenuated P301L-hTau-toxicity by reducing tau hyperphosphorylation and its pathological aggregation.

STAT3 activates the transcription of NMDAR via binding to the specific GAS promoter element

We measured the level of synapse-related protein to explore the molecular mechanisms underlying STAT3 ameliorating P301L-hTau-induced dendritic plasticity impairments. P301L-hTau accumulation or STAT3 knockdown by AAV-Cre in mice decreased the protein and mRNA levels of postsynaptic proteins N-methyl-D-aspartate receptors (NMDARs) type 1 (GluN1), GluN2A and GluN2B (Fig. 6), while overexpression of STAT3 by AAV-STAT3 *in vivo* or *in vitro* substantially restored the reduction of protein and mRNA levels of the NMDARs induced by P301L-hTau as measured by Western blotting (Fig. 6d, e, Additional file1: Figure S6a to b) and RT-PCR (Fig. 6f, Additional file 1: Figure S6c). Further studies by chromatin immunoprecipitation (CHIP) assay demonstrated that overexpression of P301L in hippocampus markedly decreased binding of STAT3 to the promoter of GluN1, GluN2A or GluN2B (Fig. 7a), and upregulating STAT3 ameliorated the reduced transcriptional activity of the NMDARs induced by P301L (Fig. 7b). These data demonstrated that STAT3 activation promoted NMDAR expression by directly binding to the promoters.

To explore how STAT3 promotes the expression of NMDARs, we screened potential binding sites of STAT3 in the promoter regions of GluN1, GluN2A and GluN2B in a transcription factor database. We found one conserved GAS promoter element for STAT3 binding in the promoter regions of GluN1, GluN2A or GluN2B, respectively. To prove whether the GAS promoter element of GluN1, GluN2A or GluN2B genes is specific for STAT3, we constructed luciferase reporters containing GAS elements on the NMDAR promoters (Fig. 7c, e, g). After co-transfection of specific GAS element reporters with STAT3 into HEK293 cells, we found that co-expression of STAT3 with GAS on NMDARs increased luciferase activity (Fig. 7d, f, h). Furthermore, expression of mutant GAS on NMDARs abolished STAT3-induced activation of luciferase activity (Fig. 7d, f, h). These data suggest that STAT3 promotes NMDARs expression by binding to the specific GAS element.

Inhibition of STAT1 acetylation does not reverse the learning and memory impairments induced by P301L-hTau

Our present data showed that acetylated STAT1 detained STAT3 in the cytoplasm and thus inhibited STAT3 activity (Fig. 2 and 3). To investigate the role of STAT1 acetylation in regulating expression of NMDARs and cognitive ability, we constructed non-acetylation STAT1-dominant negative mutant (K410/413R-STAT1) AAV (AAV-STAT1KR) virus and co-infused the virus with AAV-P301L-hTau into the hippocampal CA3 of 2-month-old C57 mice for one month. Unexpectedly, we found that, co-expression of dominant negative KR-STAT1 improved spatial learning ability (Fig. 8c), however, did not attenuate P301L-hTau-induced spatial memory deficits though spatial memory shown an improving trend (Fig. 8d to j), and LTP suppression and spine density reduction had no change compared with P301L (Fig. 8k to

n). GluN1 and GluN2A protein and mRNA levels also showed no significant change relative to those of P301L-hTau group (Additional File 1: Figure S7).

Our previous study showed that tau accumulation activated STAT1 to inhibit NMDARs transcription [24]. STAT1 acetylation inhibited STAT1 entry into the nucleus [46]. Here, transfection with K410/413R-STAT1 (STAT1KR) may not only increase STAT3 protein level in the nuclear fraction, but also promote STAT1 entry into the nucleus. To prove this hypothesis, P301L-hTau and STAT1KR plasmids were co-transferred in HEK293 cells, and whole-cell lysis and nuclear fraction were extracted. Western blotting results showed that overexpression of STAT1KR increased both exogenous and endogenous protein levels of STAT1 and its phosphorylation at Y701 (STAT1 activated form) in the nuclear fraction significantly (Additional file 1: Figure S8a, b). The luciferase assay also showed that STAT1KR increased STAT1 transcriptional activity (Additional file 1: Figure S8c). Co-overexpression STAT1KR and WT-STAT3 had no effect in the luciferase activity of NMDARs (Additional file 1: Figure S8d). These data suggested that the inhibition of STAT1 acetylation resulted in activating STAT1, which antagonized the promoting effects of STAT3 on the transcription of NMDARs.

JAK2 kinase mediates phosphorylation of STAT3 at Y705

Our previous paper reported that hTau accumulation activated tyrosine kinase JAK2, JNK and ERK, which are reported to mediate phosphorylation of the STAT family [24]. Here, we also found that P301L-hTau activated JAK2, JNK and ERK (Additional file 1: Figure S9a, b). Simultaneous inhibition of JAK2 by JAK2 inhibitor TG-101348 (JAK2I) or JAK2 siRNA but not JNK or ERK inhibitor abolished P301L-hTau-induced STAT3 phosphorylation at pY705 in the cell extracts (Additional file 1: Figure S9c to f).

Discussion

While the amount of abnormal tau protein aggregation into neurofibrillary tangles is positively correlated with the degree of neurodegeneration and memory impairment in tauopathies [5], how tau accumulation affects synaptic proteins has been unclear until now. By overexpression of P301L-hTau (P301L), the human tau with the most common FTDP-17 mutation [47], we found that P301L accumulation caused STAT3 retention in the cytoplasm by acetylating STAT1 and increasing binding with STAT3 in the cytoplasmic fraction, which inhibited the translocation of STAT3 into the nucleus, and inactivated STAT3. Knockdown of STAT3 in the $STAT3^{flox/flox}$ mice by AAV-Cre mimicked overexpressing P301L-induced synaptic and cognitive deficits via inhibition of the expression of GluN1, GluN2A, and GluN2B by binding to their specific promoter elements. We also demonstrated that overexpressing STAT3 attenuated P301L induced synaptic and cognitive deficits. These findings reveal that intracellular accumulation of P301L-hTau causes memory deterioration through suppression of NMDARs expression via inactivation of STAT3, which discloses a novel mechanism for tau-related synapse and memory impairments.

The STAT protein family includes 7 members: STAT1-4, STAT5a, STAT5b, and STAT6, which serve as transcription factors that bind to the target gene's DNA promoter region [25–27]. Our recent paper showed that overexpressing hTau upregulated STAT1 activity and inhibited the transcription of NMDARs [24]. As STAT1 and STAT3 have a similar DNA-binding domain GAS element [25, 26], here we found both *in vivo* and *in vitro* that overexpressing P301L induced STAT3 phosphorylation at tyrosine 705. The increased phosphorylated level is reported to lead STAT3 to transport from the cytoplasm into the nucleus and initiate transcription of the corresponding target gene [40, 41]. However, STAT3 in the nuclear fraction decreased, which suggested that STAT3 transport into the nucleus was inhibited by overexpressing P301L. By using multiple measures, including phosphorylation (pS727-STAT3) which regulates the transcriptional activation of STAT3 [48, 49], dimerization, EMSA, and luciferase activity assay, we provide strong evidence to show that P301L accumulation inactivates STAT3.

Phosphorylated STAT3 at Tyr705 induces not only STAT3 to form a homologous dimer but also a heterodimer with STAT1 [50, 51]. Firstly, we found that the interaction between STAT1 with STAT3 increased in the cytoplasm but decreased in the nucleus. It is reported that the acetylation of STAT1 increased the binding with NF-κB p65 and inhibited its incorporation into the nucleus [42]. By mass spectrometry, two STAT1 acetylated sites K410 and K413 were identified, and overexpressing the pseudoacetylated STAT1 mutant at both sites (K410/413Q-STAT1) decreased STAT3 in the nuclear fraction, while overexpressing the dominant negative non-acetylated STAT1 mutant at both sites (K410/413R-STAT1) attenuated the reduction of STAT3 in the nuclear fraction induced by P301L. We also found that overexpressing K410/413Q-STAT1 decreased STAT3 transcriptional activity, while overexpressing K410/413R-STAT1 ameliorated the decreased P301L-induced STAT3 activity. These data suggest that P301L overexpression acetylated STAT1 and STAT1 acetylation bound with STAT3 in the cytoplasm and thus caused STAT3 retention in the cytoplasm, finally resulted in inactivation of STAT3. We also noticed that only overexpressing K410/413R-STAT1 did not change the subcellular localization of STAT3, but it might be that the acetylated STAT1 level was at a low basal level, a subject that needs further study.

To identify the exact binding element(s) of STAT3 on NMDAR promoters, we constructed GAS promoter elements in NMDAR promoter regions for luciferase activity assay. As the specific sequence of the GAS element for STAT1 is TTC(N2-4)GAA, and for STAT3 is TTC(N3)GAA [26, 27], we observed only one conserved GAS promoter element for STAT3 binding in the promoter regions of GluN1, GluN2B or GluN2A, though there are 2 conserved GAS promoter elements for STAT1 binding in the promoter regions of GluN1 and GluN2B, and 4 GAS promoter elements in GluN2A [24]. By transfection with GAS-NMDARs or MUT-GAS-NMDARs (mutant) plasmid construct, we found that STAT3 positively regulates the luciferase activity of NMDRAs. Combined with data from Chip, PCR and Western blotting, we concluded that STAT3 positively regulates the expression of NMDARs. Though STAT1 and STAT3 both belong to the same protein family and employ similar GAS elements to regulate downstream gene expression as a transcriptional factor, we first found that STAT3 and STAT1 nevertheless have opposite regulatory roles in NMDARs expression: STAT3 positively regulates NMDARs expression, while STAT1 negatively regulates NMDARs expression [24]. This opposing role of STAT1 and STAT3 in the regulation of target genes

expression was also observed in IL-21 signaling in $CD4^+$ T cells; whereas STAT1 increased IFN-γ production, STAT3 suppressed IFN-γ expression [52].

Besides the presence of abnormal tau protein, some tau-dominated polyprotein proteinopathies contain other abnormal protein accumulations, including TDP-43 and α-synuclein. We found that neither TDP-43 nor α-synuclein affected the activity of STAT3, and they also did not change the expression of NMDARs. These negative results suggest that the inactivation of STAT3 is specific for Tau accumulation.

To investigate the mechanisms by which overexpression of P301L induced an increase of STAT1 acetylation, we used the proteins CBP, p300 or HDAC2, which have acetylase or deacetylase activity [42–44]. However, only CBP protein level was significantly decreased in P301L overexpression, which suggests that CBP, p300 or HDAC2 are not involved in STAT1 acetylation. Tau protein itself has been reported to possess acetyltransferase activity, such that the repeat domain K18 mediates the acetyl transferase action [45]. We found that P301L interacted with STAT1 and thus increased the STAT1 acetylation level, but overexpressing K18(-) (K18-deleted P301L mutant) had no effects on the acetylated level of STAT1. These *in vitro* and *in vivo* data suggested that P301L accumulation acetylated STAT1. We also found that here, similar to our earlier demonstration that hTau accumulation activated JAK2 [24], that P301L also activated JAK2 to phosphorylate STAT3. This implies that activation of JAK2/STAT signaling pathway is a common effect of Tau accumulation.

As STAT1 acetylation played a key role in the nuclear localization and transcriptional activity of STAT3, we infected AAV-STAT1KR (410/413R-STAT1) with AAV-P301L virus into C57 mice and investigated whether non-acetylated STAT1 overexpression attenuated P301L-induced synaptic and cognitive deficits. Unexpectedly, overexpression of STAT1KR had no effect on the P301L-induced impairment of dendritic plasticity and memory ability. This was the result of inhibition of STAT1 acetylation promoted STAT3 transport into the nucleus and activation of STAT3, while STAT1 in the nuclear fraction and its activity was also increased by non-acetylated STAT1. We recently reported that STAT1 negatively regulates the expression of NMDARs [24]. The negative effects of STAT1 activation antagonized the positive effects of STAT3 activation in NMDARs expression, so NMDARs expression (mRNA and protein level) showed no change and memory also did not been improved. The reason for non-acetylated STAT1 favor STAT1 nuclear translocation is that, as a positive charge is required for STAT1 to associate with nuclear translocation, Lys410 and lys413 are embedded within the nuclear localization sequence of STAT1, such that acetylation of these lysines would neutralize their positive charge and preclude STAT1 nuclear accumulation [46, 53].

Conclusions

By combining the present data with those in our recent study [24], we propose the following ‘trade-off hypothesis’ as the molecular mechanism by which the accumulation of tau induces synaptic deficits. We propose that tau accumulation activates the JAK2/STAT1 signaling pathway to phosphorylate STAT1 at Y701, promotes STAT1 to form a homodimer for transport into the nucleus, and thus activates STAT1 to

suppress the expression of NMDARs [24]. To rectify the adverse consequences of STAT1 activation, tau acetylates STAT1 to inhibit STAT1 nuclear translocation. However, acetylated STAT1 could not prevent STAT1 nuclear translocation, but promotes STAT1 binding with STAT3 to form a heterodimer in the cytoplasm, which prevents STAT3 transport into the nucleus even though JAK2 phosphorylates STAT3 at Y705. Tau accumulation inhibits NMDARs expression via upregulation of STAT1 activity and downregulation of STAT3 activity, ultimately leading to synaptic dysfunction and cognitive deficits (Fig. 9).

Abbreviations

AD, Alzheimer's disease; FTDP-17, frontotemporal dementia; STAT1, Signal Transduction and Activator of Transcription-1; STAT3, Signal Transduction and Activator of Transcription-3; NMDAR, N-methyl-D-aspartate receptor; MWM, Morris water maze; CaMKIV, calcium/calmodulin-dependent protein kinase IV; fEPSP, excitatory postsynaptic potential; LTP, long-term potentiation; DMEM, Dulbecco's Modified Eagle's medium; LTM, Long-term memory; aCSF, artificial cerebrospinal fluid; EMSA, Electrophoresis mobility shift assay; ChIP, Chromatin immunoprecipitation;

Declarations

Ethics approval and consent to participate

All animal experiments were performed according to the 'Policies on the Use of Animals and Humans in Neuroscience Research' revised and approved by the Society for Neuroscience in 1995, and the animal study was approved by the Academic Review Board of Tongji Medical College, Huazhong University of Science and Technology.

Consent for publication

Not applicable

Availability of supporting data

The authors declare that the data supporting the findings of this study are available within the article and its Supplementary Information files, or from the authors upon **request.**

Competing interests

The authors declare that they have no competing interests.

Funding

This work was supported in parts by Natural Science Foundation of China (81870846), the Ministry of Science and Technology of China (2016YFC13058001), and Sanming Project of Medicine in Shenzhen

(SZSM201611090).

Authors' contributions

G.P.L. and X.F.Y. conceived the project, designed the experiments, and wrote the manuscript. X.Y.H, H.L.W. and X.G.L. designed and performed most of the experiments. H.L.W., T.L., and X.W. performed electrophysiological experiments. B.G.Z., X.L. and Q.L. prepared primary neurons. C.Y.C. performed the immunohistochemical experiments. Y.Y., Q.W., S.P.L and H.Y. assisted with *in vivo* and *in vitro* experiments. J.Z.W. assisted with data analysis and interpretation and critically read the manuscript. All authors read and approved the final manuscript.

Acknowledgements

We thank Dr. Xiao-Yuan Li of Institute of Biomedical Sciences, Academia Sinica, Taiwan for the kind gift of STAT1 plasmid.

Author's information

[1]Department of Pathophysiology, School of Basic Medicine and the Collaborative Innovation Center for Brain Science, Key Laboratory of Ministry of Education of China and Hubei Province for Neurological Disorders, Tongji Medical College, Huazhong University of Science and Technology, Wuhan 430030, China

[2] Clinic Center of Human Gene Research, Union Hospital, Tongji Medical College, Huazhong University of Science and Technology, China

[3]State Key Laboratory of Oncogenomics, School of Chemical Biology and Biotechnology, Peking University Shenzhen Graduate School, Shenzhen, China

[4]Bomedical Engineering, Shenzhen Polytechnic, Shenzhen, 518055, China

[5]Key Laboratory of Modern Toxicology of Shenzhen, Shenzhen Center for Disease Control and Prevention, Shenzhen 518055, China

[6]Co-innovation Center of Neuroregeneration, Nantong University, Nantong, JS 226001, China

References

1. Tolnay M, Probst A. The neuropathological spectrum of neurodegenerative tauopathies. IUBMB Life. 2003;55(6):299-305.
2. Lee VM, Trojanowski JQ. Neurodegenerative tauopathies: human disease and transgenic mouse models. Neuron. 1999; 24(3):507-10.

3. Lee VM, Goedert M, Trojanowski JQ. Neurodegenerative tauopathies. Annu Rev Neurosci. 2001; 24:1121-59.
4. Braak H, Alafuzoff I, Arzberger T, Kretzschmar H, Del Tredici K. Staging of Alzheimer disease-associated neurofibrillary pathology using paraffin sections and immunocytochemistry. Acta Neuropathol. 2006; 112(4):389-404.
5. Lin YT, Cheng JT, Yao YC, Juo, Lo YK, Lin CH, Ger LP, et al. Increased total TAU but not amyloid-beta(42) in cerebrospinal fluid correlates with short-term memory impairment in Alzheimer's disease. J Alzheimers Dis. 2009;18(4):907-18.
6. Hu YY, He SS, Wang X, Duan QH, Grundke-Iqbal I, Iqbal K, et al. Levels of nonphosphorylated and phosphorylated tau in cerebrospinal fluid of Alzheimer's disease patients: an ultrasensitive bienzyme-substrate-recycle enzyme-linked immunosorbent assay. Am J Pathol. 2002; 160(4): 1269-78.
7. Lewis J, McGowan E, Rockwood J, Melrose H, Nacharaju P, Van Slegtenhorst M, et al. Neurofibrillary tangles, amyotrophy and progressive motor disturbance in mice expressing mutant (P301L) tau protein. Nat Genet. 2000; 25(4):402-5.
8. Götz J, Deters N, Doldissen A, Bokhari L, Ke Y, Wiesner A, et al. A decade of tau transgenic animal models and beyond. Brain Pathol. 2007; 17(1):91-103.
9. Kimura T, Yamashita S, Fukuda T, Park JM, Murayama M, Mizoroki T, et al. Hyperphosphorylated tau in parahippocampal cortex impairs place learning in aged mice expressing wild-type human tau. EMBO J. 2007; 26(24):5143-52.
10. Boutajangout A, Quartermain D, Sigurdsson EM. Immunotherapy targeting pathological tau prevents cognitive decline in a new tangle mouse model. J Neurosci. 2010; 30(49):16559-66.
11. Roberson ED, Scearce-Levie K, Palop JJ, Yan F, Cheng IH, Wu T, et al. Reducing endogenous tau ameliorates amyloid beta-induced deficits in an Alzheimer's disease mouse model. Science. 2007; 316(5825):750-4.
12. Ittner LM, Ke YD, Delerue F, Bi M, Gladbach A, van Eersel J, et al. Dendritic function of tau mediates amyloid-beta toxicity in Alzheimer's disease mouse models. Cell. 2010; 142(3):387-97.
13. Vossel KA, Zhang K, Brodbeck J, Daub AC, Sharma P, Finkbeiner S, et al. Tau reduction prevents Abeta-induced defects in axonal transport. Science. 2010; 330(6001):198.
14. Ittner A, Chua SW, Bertz J, Volkerling A, van der Hoven J, Gladbach A, et al. Site-specific phosphorylation of tau inhibits amyloid-β toxicity in Alzheimer's mice. Science. 2016; 354(6314): 904-8.
15. Alonso AC, Zaidi T, Grundke-Iqbal I, Iqbal K. Role of abnormally phosphorylated tau in the breakdown of microtubules in Alzheimer disease. Proc Natl Acad Sci U S A. 1994; 91(12): 5562-6.
16. Ebneth A, Godemann R, Stamer K, Illenberger S, Trinczek B, Mandelkow E. Overexpression of tau protein inhibits kinesin-dependent trafficking of vesicles, mitochondria, and endoplasmic reticulum: implications for Alzheimer's disease. J Cell Biol. 1998;143(3):777-94.
17. Li HL, Wang HH, Liu SJ, Deng YQ, Zhang YJ, Tian Q, et al. Phosphorylation of tau antagonizes apoptosis by stabilizing beta-catenin, a mechanism involved in Alzheimer's neurodegeneration. Proc

Natl Acad Sci U S A. 2007; 104(9):3591-6.

18. Duan DX, Chai GS, Ni ZF, Hu Y, Luo Y, Cheng XS, et al. Phosphorylation of tau by death-associated protein kinase 1 antagonizes the kinase-induced cell apoptosis. J Alzheimers Dis. 2013; 37(4):795-808.
19. Luo DJ, Feng Q, Wang ZH, Sun DS, Wang Q, Wang JZ, et al. Knockdown of phosphotyrosyl phosphatase activator induces apoptosis via mitochondrial pathway and the attenuation by simultaneous tau hyperphosphorylation. J Neurochem. 2014; 130(6):816-25.
20. Hu Y, Li XC, Wang ZH, Luo Y, Zhang X, Liu XP, et al. Tau accumulation impairs mitophagy via increasing mitochondrial membrane potential and reducing mitochondrial Parkin. Oncotarget. 2016; 7(14):17356-68.
21. Li XC, Hu Y, Wang ZH, Luo Y, Zhang Y, Liu XP, et al. Human wild-type full-length tau accumulation disrupts mitochondrial dynamics and the functions via increasing mitofusins. Sci Rep. 2016; 6:24756.
22. Yin Y, Gao D, Wang Y, Wang ZH, Wang X, Ye J, et al. Tau accumulation induces synaptic impairment and memory deficit by calcineurin-mediated inactivation of nuclear CaMKIV/CREB signaling. Proc Natl Acad Sci U S A. 2016; 113(26):E3773-81.
23. Feng Q, Luo Y, Zhang XN, Yang XF, Hong XY, Sun DS, et al. MAPT/Tau accumulation represses autophagy flux by disrupting IST1-regulated ESCRT-III complex formation: a vicious cycle in Alzheimer neurodegeneration. Autophagy. 2020;16(4):641-58.
24. Li XG, Hong XY, Wang YL, Zhang SJ, Zhang JF, Li XC, et al. Tau accumulation triggers STAT1-dependent memory deficits by suppressing NMDA receptor expression. EMBO Rep. 2019; 20(6): pii: e47202.
25. Darnell JE Jr. STATs and gene regulation. Science. 1997; 277(5332):1630-5.
26. Lim CP, Cao X. Structure, function, and regulation of STAT proteins. Mol Biosyst. 2006; 2(11): 536-50.
27. Xu L, Ji JJ, Le W, Xu YS, Dou D, Pan J, et al. The STAT3 HIES mutation is a gain-of-function mutation that activates genes via AGG-element carrying promoters. Nucleic Acids Res. 2015; 43(18): 8898-912.
28. Hsu WL, Ma YL, Hsieh DY, Liu YC, Lee EH. STAT1 negatively regulates spatial memory formation and mediates the memory-impairing effect of Aβ. Neuropsychopharmacology. 2014; 39(3): 746-58.
29. Tai DJ, Hsu WL, Liu YC, Ma YL, Lee EH. Novel role and mechanism of protein inhibitor of activated STAT1 in spatial learning. EMBO J. 2011; 30(1):205-20.
30. Park SJ, Shin EJ, Min SS, An J, Li Z, Hee Chung Y, et al. Inactivation of JAK2/STAT3 signaling axis and downregulation of M1 mAChR cause cognitive impairment in klotho mutant mice, a genetic model of aging. Neuropsychopharmacology. 2013;38(8):1426-37.
31. Yamada M, Chiba T, Sasabe J, Terashita K, Aiso S, Matsuoka M. Nasal Colivelin treatment ameliorates memory impairment related to Alzheimer's disease. Neuropsychopharmacology. 2008; 33(8):2020-32.

32. Chiba T, Yamada M, Sasabe J, Terashita K, Shimoda M, Matsuoka M, et al. Amyloid-beta causes memory impairment by disturbing the JAK2/STAT3 axis in hippocampal neurons. Mol Psychiatry. 2009; 14(2):206-22.
33. Deters N, Ittner LM, Götz J. Divergent phosphorylation pattern of tau in P301L tau transgenic mice. Eur J Neurosci. 2008; 28(1):137-47.
34. Morris RG, Garrud P, Rawlins JN, O'Keefe J. Place navigation impaired in rats with hippocampal lesions. Nature. 1982; 297(5868):681-3.
35. Jiang X, Chai GS, Wang ZH, Hu Y, Li XG, Ma ZW, et al. CaMKII-dependent dendrite ramification and spine generation promote spatial training-induced memory improvement in a rat model of sporadic Alzheimer's disease. Neurobiol Aging. 2015; 36(2):867-76.
36. Morrone CD, Bazzigaluppi P, Beckett TL, Hill ME, Koletar MM, Stefanovic B, et al. Regional differences in Alzheimer's disease pathology confound behavioural rescue after amyloid-β attenuation. Brain. 2019; 143(1):359-73.
37. Fernandes HB, Riordan S, Nomura T, Remmers CL, Kraniotis S, Marshall JJ, et al. Epac2 mediates cAMP-dependent potentiation of neurotransmission in the hippocampus. J Neurosci. 2015; 35(16):6544-53.
38. Wang H, Ardiles AO, Yang S, Tran T, Posada-Duque R, Valdivia G, et al. Metabotropic glutamate receptors induce a form of LTP controlled by translation and Arc signaling in the hippocampus. J Neurosci. 2016; 36(5):1723-9.
39. Koshelnick Y, Ehart M, Hufnagl P, Heinrich PC, Binder BR. Urokinase receptor is associated with the components of the JAK1/STAT1 signaling pathway and leads to activation of this pathway upon receptor clustering in the human kidney epithelial tumor cell line TCL-598. J Biol Chem. 1997; 272(45):28563-7.
40. Darnell JE Jr, Kerr IM, Stark GR. Jak-STAT pathways and transcriptional activation in response to IFNs and other extracellular signaling proteins. Science. 1994; 264(5164):1415-21.
41. Ihle JN. Cytokine receptor signalling. Nature. 1995;377(6550):591-4.
42. Krämer OH, Baus D, Knauer SK, Stein S, Jäger E, Stauber RH, et al. Acetylation of Stat1 modulates NF-kappaB activity. Genes Dev. 2006; 20(4):473-85.
43. Chan HM, La Thangue NB. p300/CBP proteins: HATs for transcriptional bridges and scaffolds. J Cell Sci. 2001; 114(Pt 13):2363-73.
44. de Ruijter AJ, van Gennip AH, Caron HN, Kemp S, van Kuilenburg AB. Histone deacetylases (HDACs): characterization of the classical HDAC family. Biochem J. 2003; 370(Pt 3):737-49.
45. Cohen TJ, Friedmann D, Hwang AW, Marmorstein R, Lee VM. The microtubule-associated tau protein has intrinsic acetyltransferase activity. Nat Struct Mol Biol. 2013; 20(6):756-62.
46. Zhuang S. Regulation of STAT signaling by acetylation. Cell Signal. 2013;25(9):1924-31.
47. Götz J, Chen F, Barmettler R, Nitsch RM. Tau filament formation in transgenic mice expressing P301L tau. J Biol Chem. 2001; 276(1):529-34.

48. Wen Z, Zhong Z, Darnell JE Jr. Maximal activation of transcription by Stat1 and Stat3 requires both tyrosine and serine phosphorylation. Cell. 1995; 82(2):241-50.
49. Yokogami K, Wakisaka S, Avruch J, Reeves SA. Serine phosphorylation and maximal activation of STAT3 during CNTF signaling is mediated by the rapamycin target mTOR. Curr Biol. 2000; 10(1): 47-50.
50. Shuai K, Liu B. Regulation of JAK-STAT signalling in the immune system. Nat Rev Immunol. 2003; 3(11):900-11.
51. Levy DE, Darnell JE Jr. Stats: transcriptional control and biological impact. Nat Rev Mol Cell Biol. 2002; 3(9):651-62.
52. Wan CK, Andraski AB, Spolski R, Li P, Kazemian M, Oh J, et al. Opposing roles of STAT1 and STAT3 in IL-21 function in CD4+ T cells. Proc Natl Acad Sci U S A. 2015; 112(30):9394-9.
53. Krämer OH, Heinzel T. Phosphorylation-acetylation switch in the regulation of STAT1 signaling. Mol Cell Endocrinol. 2010; 315(1-2):40-8.

Figures

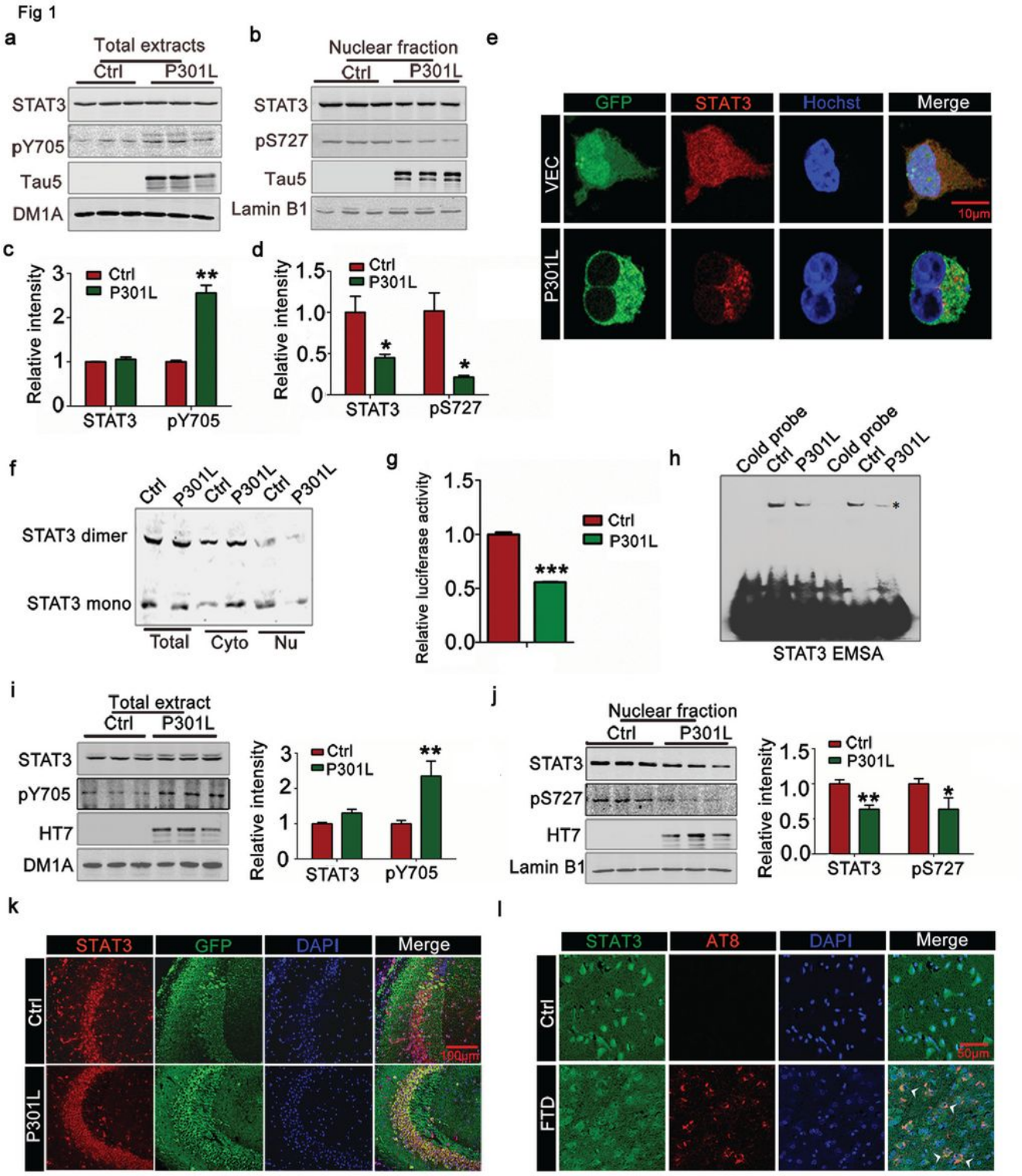

Figure 1

Intracellular P301L-hTau accumulation inactivates STAT3 via inhibition of nuclear translocation. (a-d) Overexpression of human tau containing the most common FTDP-17 mutation (P301L-hTau, or P301L) increased phosphorylated STAT3 at Tyr705 (pY705) in whole-cell extracts (a) and decreased total STAT3 and STAT3 phosphorylated at Ser727 (pS727) in the nuclear fraction (b) detected by Western blotting and quantitative analysis (c, d) (n=4). The empty vector was transfected as a control (Ctrl). (e) The

representative immunofluorescent images of STAT3 in HEK293 cells. (f) Overexpressing P301L significantly decreased STAT3 monomer and dimer formation in nuclear fraction (Nu), as determined by Western blotting. Cyto: cytoplasmic fraction. (g) Overexpressing P301L decreased STAT3 transcriptional activity relative to the vector control in HEK293 cells detected by luciferase assay (n=5). (h) Overexpressing P301L decreased STAT3-DNA-binding activity in HEK293 cells measured by electrophoretic mobility shift assay (EMSA). * indicates STAT3/DNA complex. (i, j) AAV-P301L-hTau-eGFP (AAV-P301L) or the empty vector AAV-eGFP (1.3×1013 v.g./ml) was stereotaxically injected into hipocampal CA3 of 2-month-old C57 mice for 1 month. The increased phosphorylated level of STAT3 (pY705) in hippocampal total extracts (i) and decreased total and phosphorylated STAT3 (pS727) in the nuclear fraction (j) in P301L group, were measured by Western blotting and quantitative analysis (n=4). (k) The representative immunofluorescent images of STAT3 in hippocampal CA3 region after transfection with virus for 1 month. (l) The representative immunofluorescent images of STAT3 in FTDP-17 patients. Data were presented as mean±SD (Mann-Whitney test). *, $p<0.05$, **, $p<0.001$, **, $p<0.0001$ vs Ctrl.

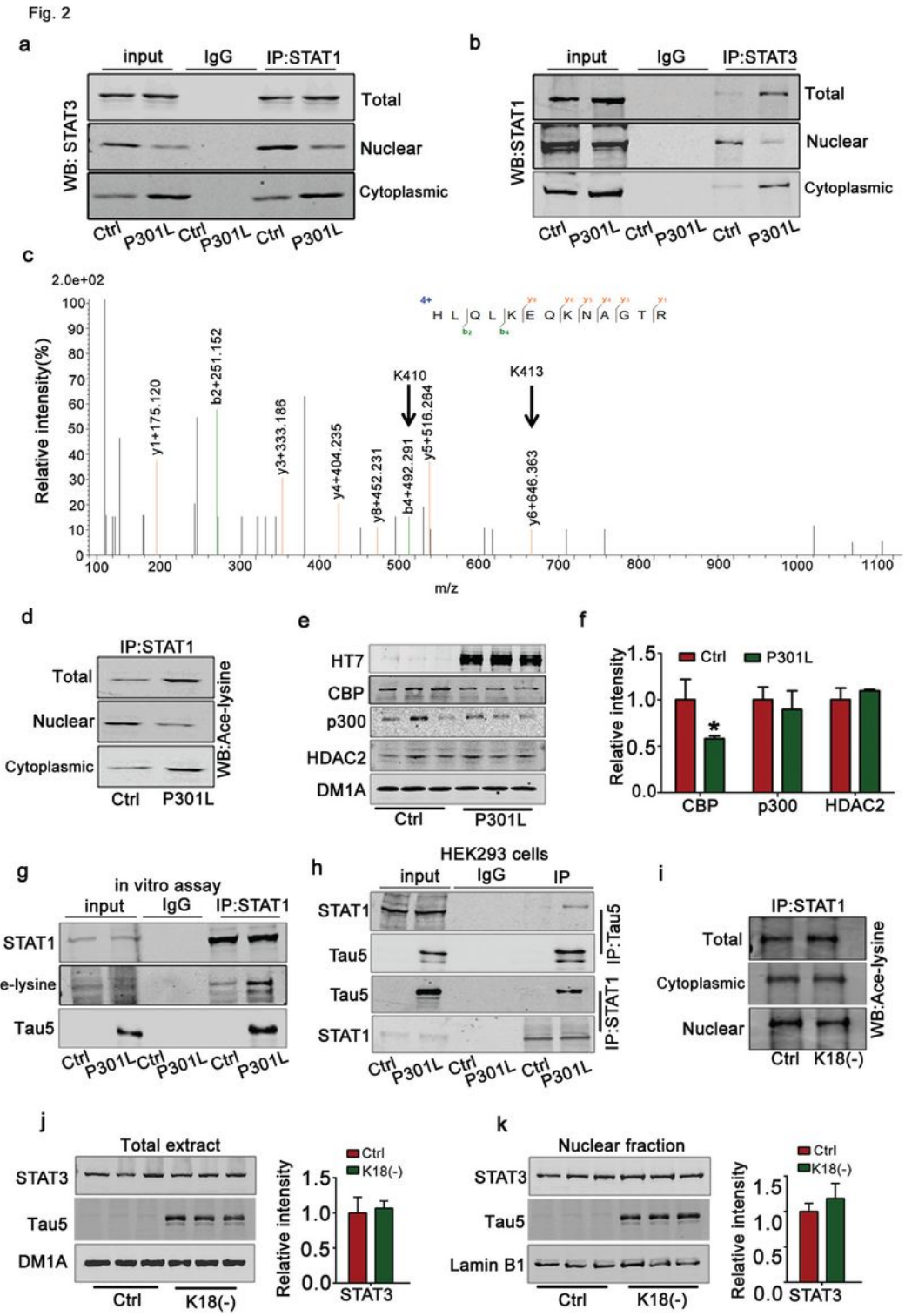

Figure 2

Overexpression of P301L-hTau increases acetylated level of STAT1 by tau acetyltransferase activity. (a, b) Overexpression of P301L increased the interaction of STAT1 and STAT3 in the cytoplasmic fraction of HEK293 cells measured by CO-IP. (c) Mass spectrometry analysis of the acetylated peptide of STAT1. The detected MS/MS peptide spectra are listed. (d) Overexpression of P301L increased the level of STAT1 acetylation in whole-cell extracts and the cytoplasm. Proteins were first immunoprecipitated with STAT1,

followed by Western blotting with anti-ace-lysine antibody. (e, f) The CBP level decreased, and p300 and HDAC2 level remained unchanged while overexpressing P301L in HEK293 cells detected by Western blotting. (g) The P301L-hTau recombinant protein interacted with STAT1 and increased its acetylation level in the whole extracts of HEK293WT cells. (h) Tau interacted with STAT1 in HEK293WT cells transfected with P301L-hTau detected by Co-IP assay. (i) P301L-K18(-) (P301L tau lacking the repeats) had no effect on acetylated STAT1 level. (j, k) P301L-K18(-) (P301L tau lacking the repeats) had no effect on STAT3 levels in total extracts (j) or the nuclear fraction (k) measured by Western blotting and quantitative analysis. Data were presented as mean ±SD (Mann-Whitney test). *, p<0.05 vs Ctrl.

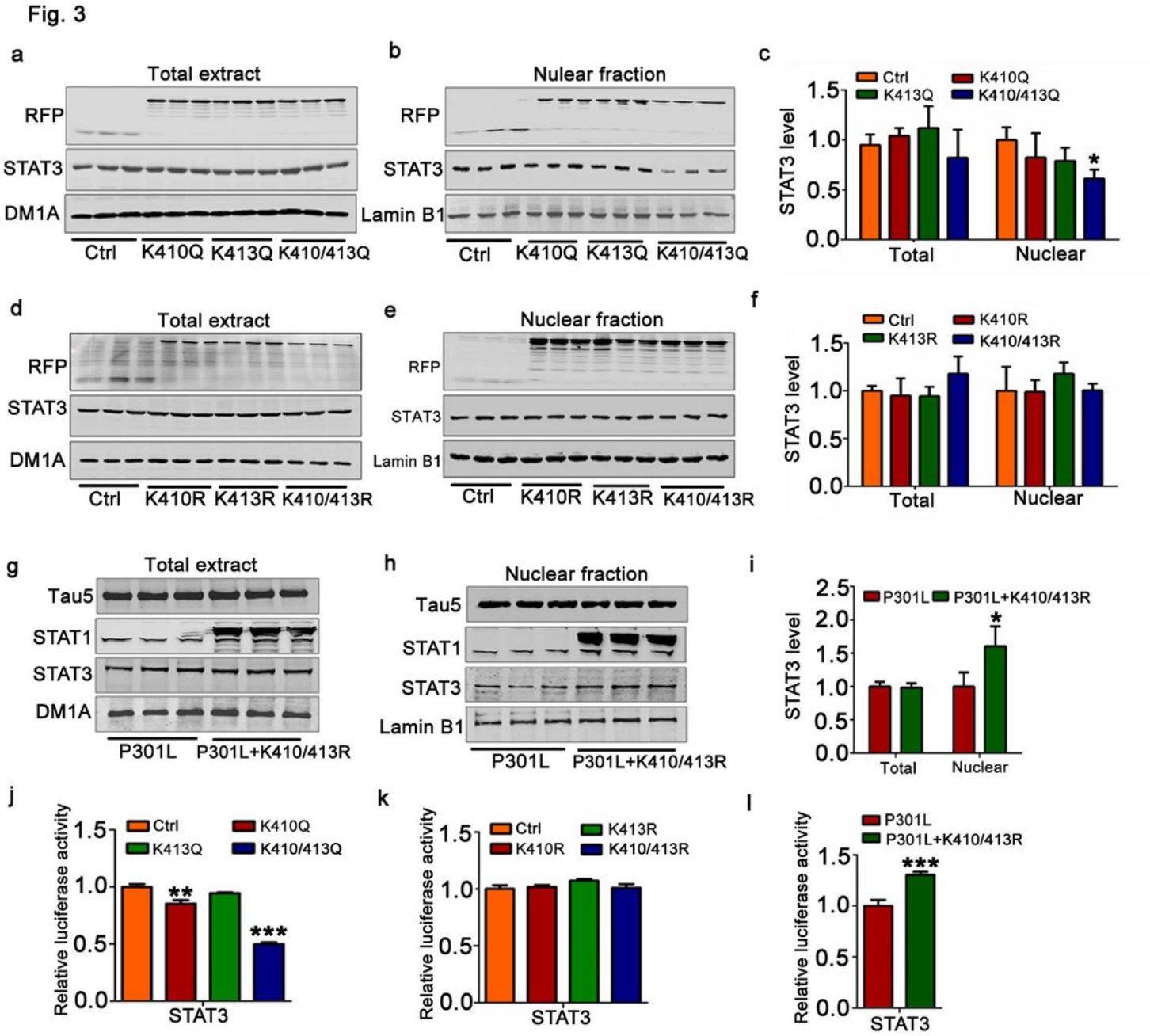

Figure 3

Acetylated STAT1 inhibited STAT3 nuclear translocation (a-c) Pseudoacetylated STAT1 mutant (K410/413Q) decreased total STAT3 in the nuclear fraction (b) but had no effect on the total STAT3 level in the whole extracts of HEK293 cells (a) detected by Western blotting and quantitative analysis (c). (d-f) The unacetylated (K410R, K413R, K410/413R) STAT1 mutant did not change STAT3 levels in total extracts (d) or the nuclear fraction (e), as determined by Western blotting and quantitative analysis (f). (g-i) K410/K413R-STAT1 (K410/413R) restored P301L-induced reduction of decreased STAT3 in the nuclear fraction, as determined by Western blotting (g, h) and quantitative analysis (i). (j) K410/K413Q-STAT1 decreased the luciferase activity of STAT3. (k) Unacetylated (K410R, K413R, K410/413R) STAT1 mutant did not affect the luciferase activity of STAT3. (l) STAT1KR (K410/413R) rescued the decreased luciferase activity of STAT3 induced by P301L-hTau. Data were presented as mean±SD (one-way analysis of variance (ANOVA) followed by Bonferroni's post hoc test for c, f, j, and k; Mann-Whitney test for i and l; n=4). *, $p<0.05$, **, $p<0.01$, ***$p<0.001$ vs Ctrl or P301L-hTau

Fig. 4

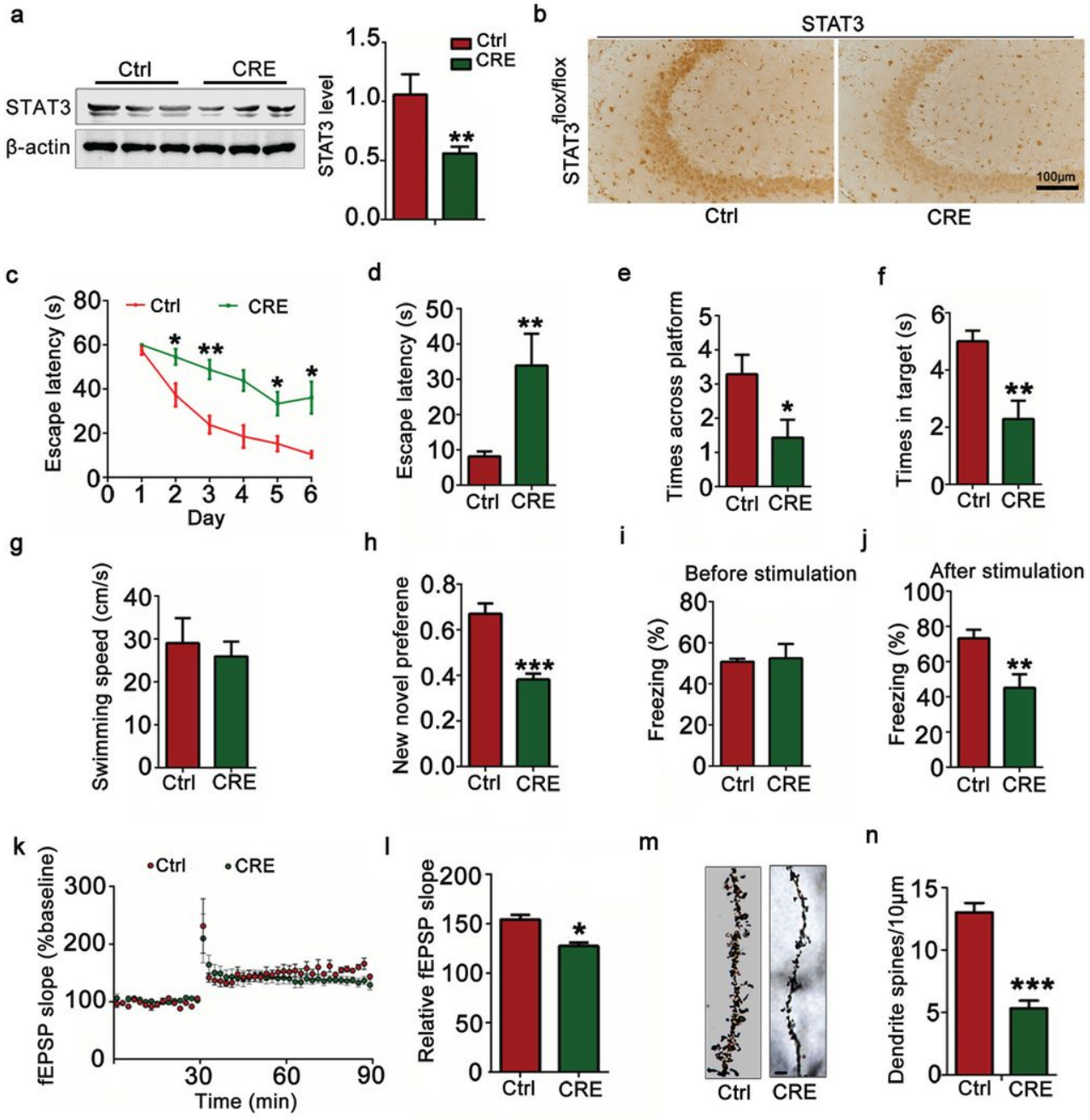

Figure 4

Downregulation of STAT3 induced synaptic impairments and memory deficits in STAT3flox/flox mice (a, b) AAV-Cre (5×1012 v.g./ml) were stereotaxically injected into the hippocampal CA3 of 2-month-old STAT3flox/flox mice. One month later, downregulation of STAT3 was confirmed by Western blotting (a) and immunohistochemical staining (b). n=4. (c) STAT3 knockdown induced spatial learning deficits shown by the increased escape latency during Morris Water Maze (MWM) training (n=8-10 for each group). (d-g) STAT3 knockdown induced spatial memory deficits shown by the increased escape latency

to reach the platform quadrant (d), the decreased crossing time in the platform site (e) and time spent in the target quadrant (f) measured at day 7 by removal of the platform in MWM test; no motor dysfunction was seen (g) (n=9-11 for each group). (h) STAT3 knockdown induced cognition impairment shown by the increased time spent in exploring the new novel object (n=8-10 for each group). (i, j) STAT3 knockdown impaired long-term memory as shown by the decreased freezing time measured in the fear conditioning test (n=8-10 each group). (k, l) STAT3 knockdown decreased slopes of field excitatory postsynaptic potentials (fEPSP, k) recorded in hippocampal CA3, and quantitative analysis (l). (n=6 slices from 4 mice for each group). (m, n) STAT3 knockdown decreased the density of dendritic spines detected by Golgi staining. Scale bar, 5μm. Data were presented as mean ±SD or mean ±SEM (Mann-Whitney test). *, $p<0.05$, **, $p<0.01$, ***, $p<0.001$ vs Ctrl.

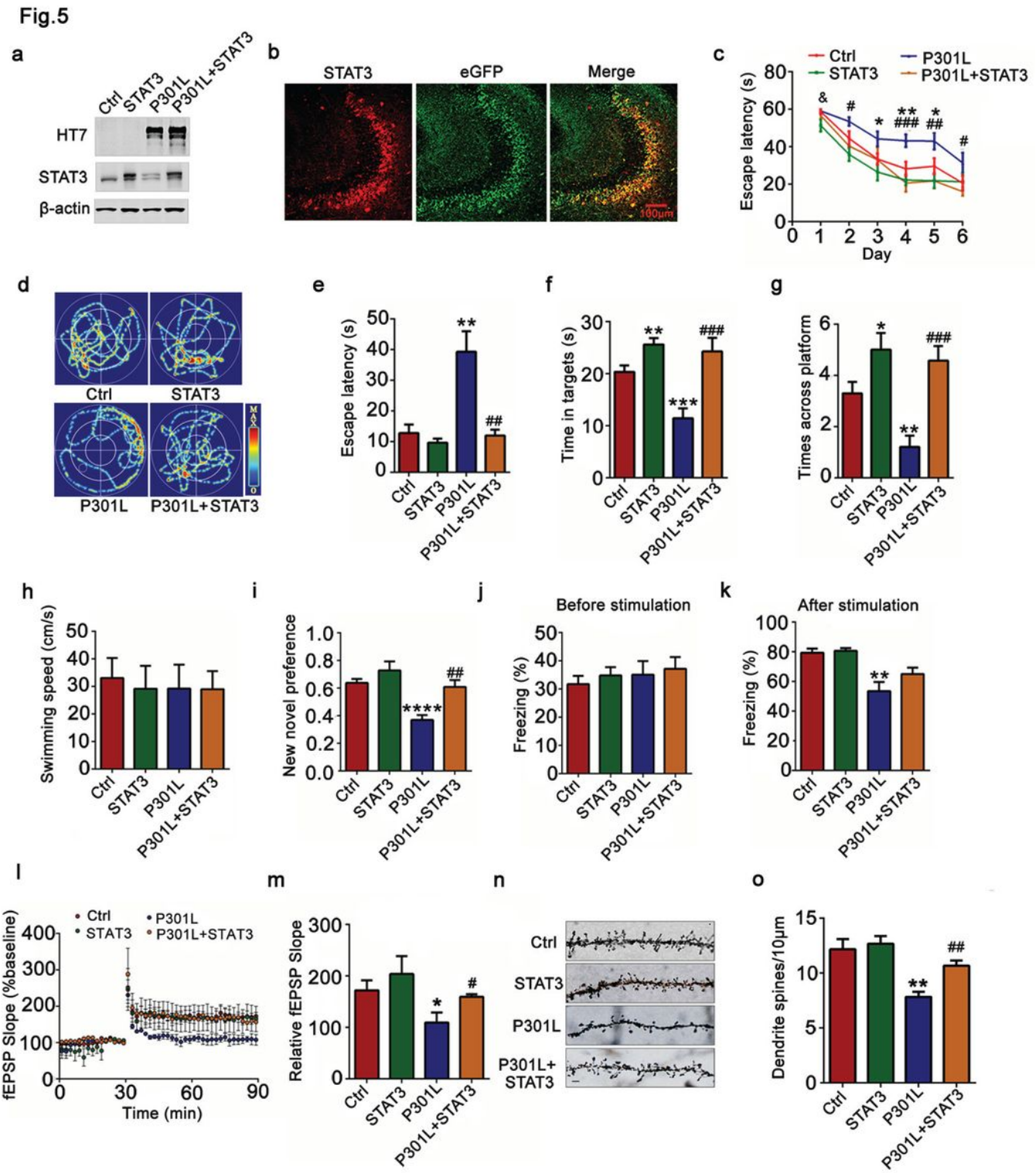

Figure 5

Overexpression of STAT3 ameliorates P301L-induced synaptic impairments and memory deficits. AAV-P301L-hTau-eGFP (P301L, 1.3×1013 v.g./ml) with or without AAV-STAT3 (1.2×1013 v.g./ml) were stereotaxically injected into hippocampal CA3 of 2-month-old C57 mice. Learning and memory ability and synaptic plasticity were assessed 1 month later. (a, b) Upregulation of STAT3 was confirmed by Western blotting (a) and immunohistochemical staining (b). (c) Upregulation of STAT3 ameliorated P301L-

induced spatial learning deficits shown by the decreased escape latency during 6 consecutive days training in Morris water maze (MWM) test (n=9-11 for each group). (d-h) Upregulation of STAT3 ameliorated hTau-induced spatial memory deficits as shown by the representative swimming trace of the mice during memory test (d), the decreased latency to reach the platform quadrant (e), the increased time spent in the target quadrant (f) and increased crossing times in the platform site (g) measured at day 7 by removing the platform in the MWM test; no motor dysfunction was seen (h) (n=9-11 for each group). (i) Upregulation of STAT3 ameliorated P301L-induced cognitive impairment as shown by the increased time spent in exploring the new novel object measured at 24 h (n=8 each group). (j, k) Upregulation of STAT3 ameliorated P301L-induced contextual memory deficits measured at 24 h during the contextual fear conditioning test (n=8 each group). (l, m) Overexpression of STAT3 restored slopes of field excitatory postsynaptic potentials (fEPSP, l) recorded in hippocampal CA3, with quantitative analysis thereof (m). (n=6 slices from 4 mice for each group). (n, o) Overexpression of STAT3 restored the density of dendritic spine detected by Golgi staining. Representative image (n) and quantitative analysis (o). Scale bar, 5μm. Data were presented as mean ±SD or mean ±SEM (two-way repeated measures analysis of variance (ANOVA) followed by Bonferroni's post hoc test for c, two-way analysis of variance (ANOVA) followed by Bonferroni's post hoc test for l, one-way analysis of variance (ANOVA) followed by Bonferroni's post hoc test for others). *, $p<0.05$, **, $p<0.01$, ***, $p<0.001$ vs Ctrl; #, $p<0.05$, ##, $p<0.01$, ###, $p<0.001$ vs P301L.

Fig. 6

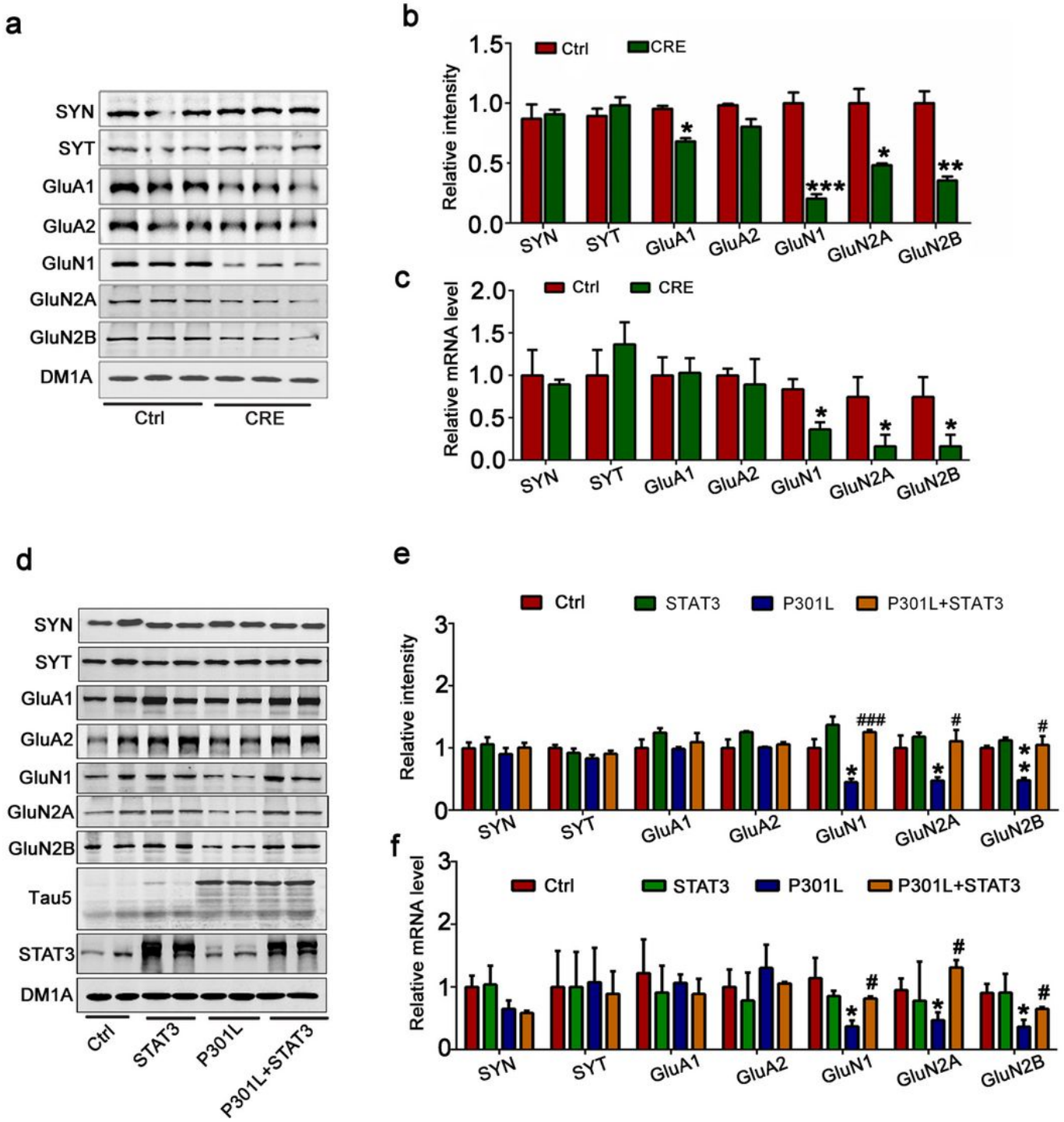

Figure 6

STAT3 positive regulates expression of NMDARs. (a-c) AAV-Cre (5×1012 v.g./ml) were stereotaxically injected into the hippocampal CA3 of 2-month-old STAT3flox/flox mice. One month later, knockout of STAT3 decreased the protein (a, b) and mRNA (c) levels of GluN1, GluN2A and GluN2B, as detected by Western blotting or qRT-PCR. (d-f) Overexpression of STAT3 ameliorated AAV-P301L-induced protein and the mRNA levels of GluN1, GluN2A and GluN2B, as detected by Western blotting or qRT-PCR in the

hippocampal CA3. Data were presented as mean ± SD (n=5; Mann-Whitney test for b and c; one-way analysis of variance (ANOVA) followed by Bonferroni's post hoc test for e and f). *, p<0.05, **, p<0.01, ***, p<0.001 vs Ctrl; #, p<0.05, ###, p<0.001 vs P301L.

Fig. 7

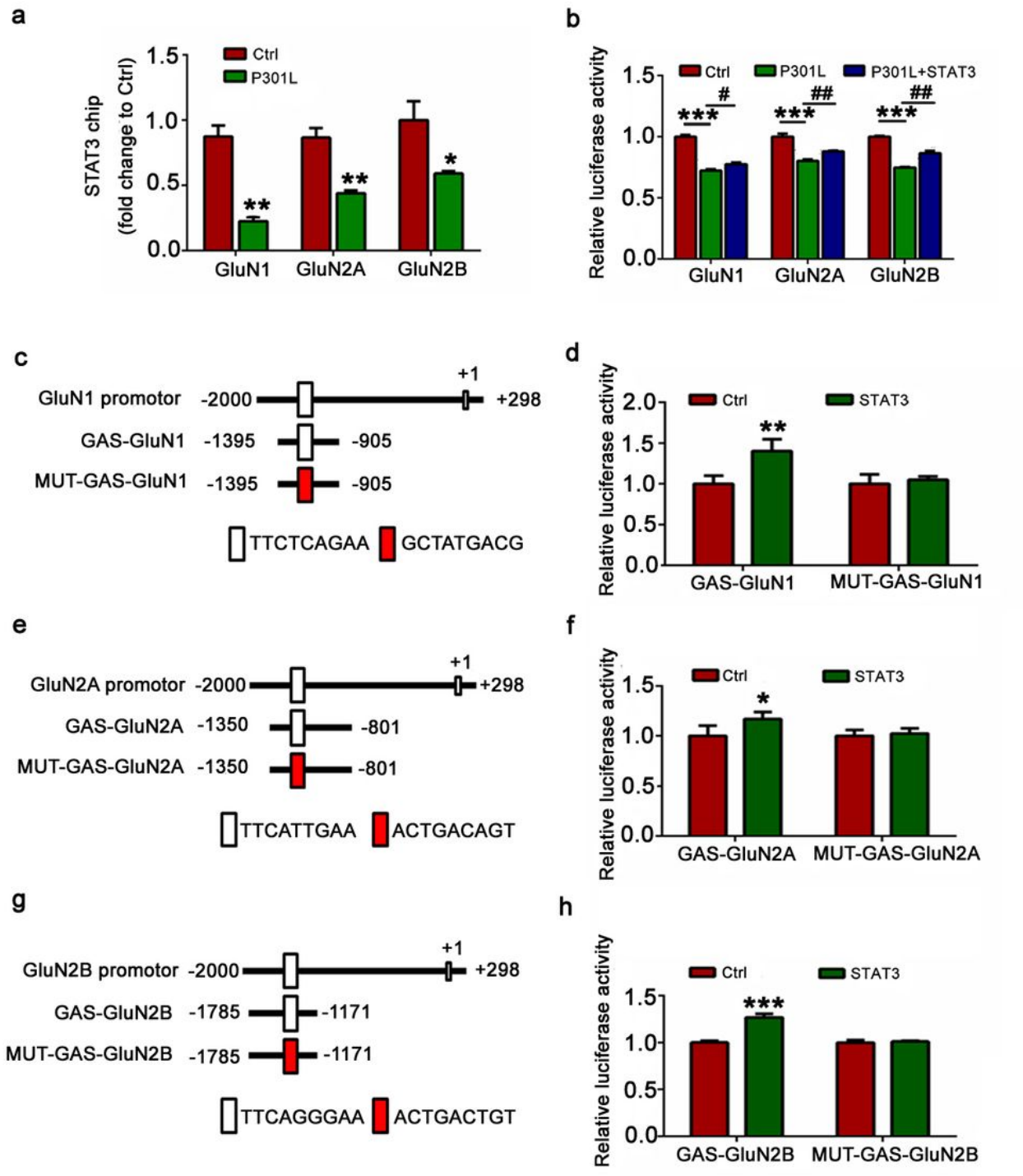

Figure 7

STAT3 binds to NMDAR promoters and promotes the expression of NMDARs. (a) Overexpression of AAV-P301L decreased binding of STAT3 to the promoter regions of GluN1, GluN2A and GluN2B genes in

hippocampal CA3 extracts, as measured by chromatin immunoprecipitation assay (ChIP) (n=4 from three independent experiments). (b) Overexpression of wild-type STAT3 (WT-STAT3) ameliorated P301L-induced reduction of the transcription activity of NMDARs, as measured by luciferase activity assay in HEK293 cells. (n=4 from three independent experiments) (c-h Diagrams show the predicted GAS promoter element (GASs) for STAT3 in the promoter (-2000-+298bp) of GluN1 (c), GluN2B (e) and GluN2A (g). The GAS or the mutant (MUT) plasmids were co-transfected respectively with WT-STAT3 or its empty vector (Ctrl) into HEK293 cells for 24 h, and then the luciferase activity was measured (right panels, d, f, h). N=4 for each group. Data were presented as mean ± SD (two-way analysis of variance (ANOVA) followed by Bonferroni' s post hoc test for b, Mann-Whitney test for others). *, $p<0.05$, **, $p<0.01$, ***, $p<0.001$ vs Ctrl; #, $p<0.05$, ##, $p<0.001$ vs P301L.

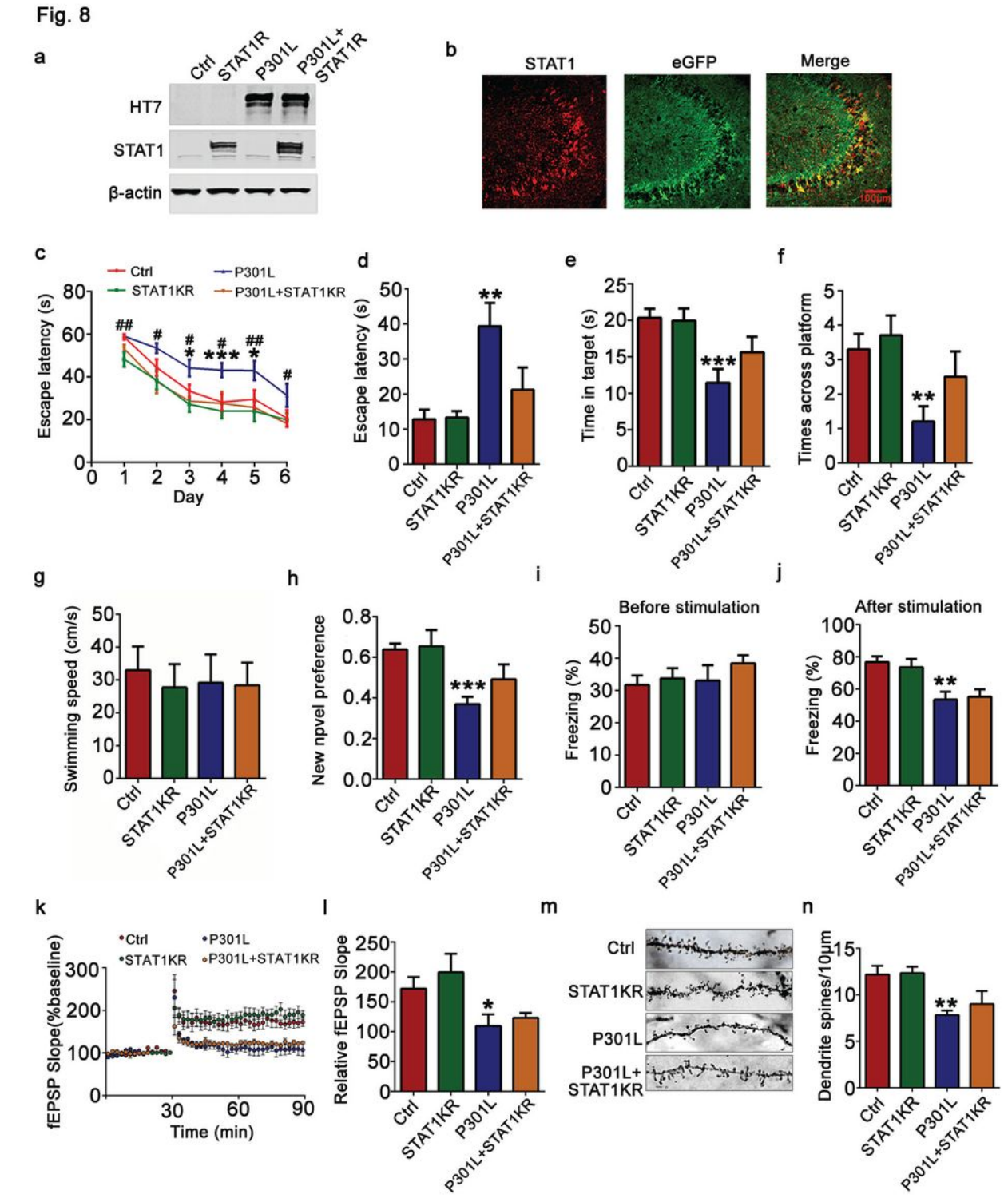

Figure 8

Inhibition of STAT1 acetylation does not ameliorate P301L-hTau-induced synaptic impairment and memory deficits. AAV-P301L-hTau-eGFP (P301L, 1.3□1013 v.g./ml) with AAV-K410/413R-STAT1 (STAT1KR, 1.1□1013 v.g./ml) were stereotaxically injected into the hippocampal CA3 of 2-month-old C57 mice. The learning and memory were detected 1 month later. (a, b) Upregulation of STAT1KR was confirmed by Western blotting and immunofluorescence staining. (c) Inhibition of STAT1 acetylation

ameliorated P301L-induced spatial learning deficits, as shown by the decrease escape latency during MWM training (n=8-10 for each group). (d-g) Inhibition of STAT1 acetylation did not ameliorate P301L-induced spatial learning deficits as shown by the unaltered escape latency to reach the platform quadrant (d), the unaltered time spent in the target quadrant (e), the unaltered times to cross the platform (f), as measured at day 8 by removing the platform. No motor dysfunction was seen (g) (n=8-10 for each group). (h) Inhibition of STAT1 acetylation did not ameliorate P301L-induced cognition impairment, as shown by the lack of variability in time spent in exploring the new novel (n=8-10 for each group). (i, j) Inhibition of STAT1 acetylation did not ameliorate P301L-induced long-term memory deficits, as shown by the invariable freezing time measured by fear conditioning test (n=8-10 each group). (k, l) Inhibition of STAT1 did not restore slopes of field excitatory postsynaptic potential (fEPSP,) recorded in hippocampal CA3, with quantitative analysis (n=5 slices from 3 mice for each group). (m, n) Golgi staining showed that the density of dendritic spine remained unaltered. Scale bars, 5μm. Data were presented as mean ±SD or mean ±SEM (two-way repeated measures analysis of variance (ANOVA) followed by Bonferroni's post hoc test for c, one-way analysis of variance (ANOVA) followed by Bonferroni's post hoc test for others). *, $p<0.05$, **, $p<0.01$, ***, $p<0.001$ vs Ctrl; #, $p<0.05$, ##, $p<0.01$ vs P301L.

Fig. 9

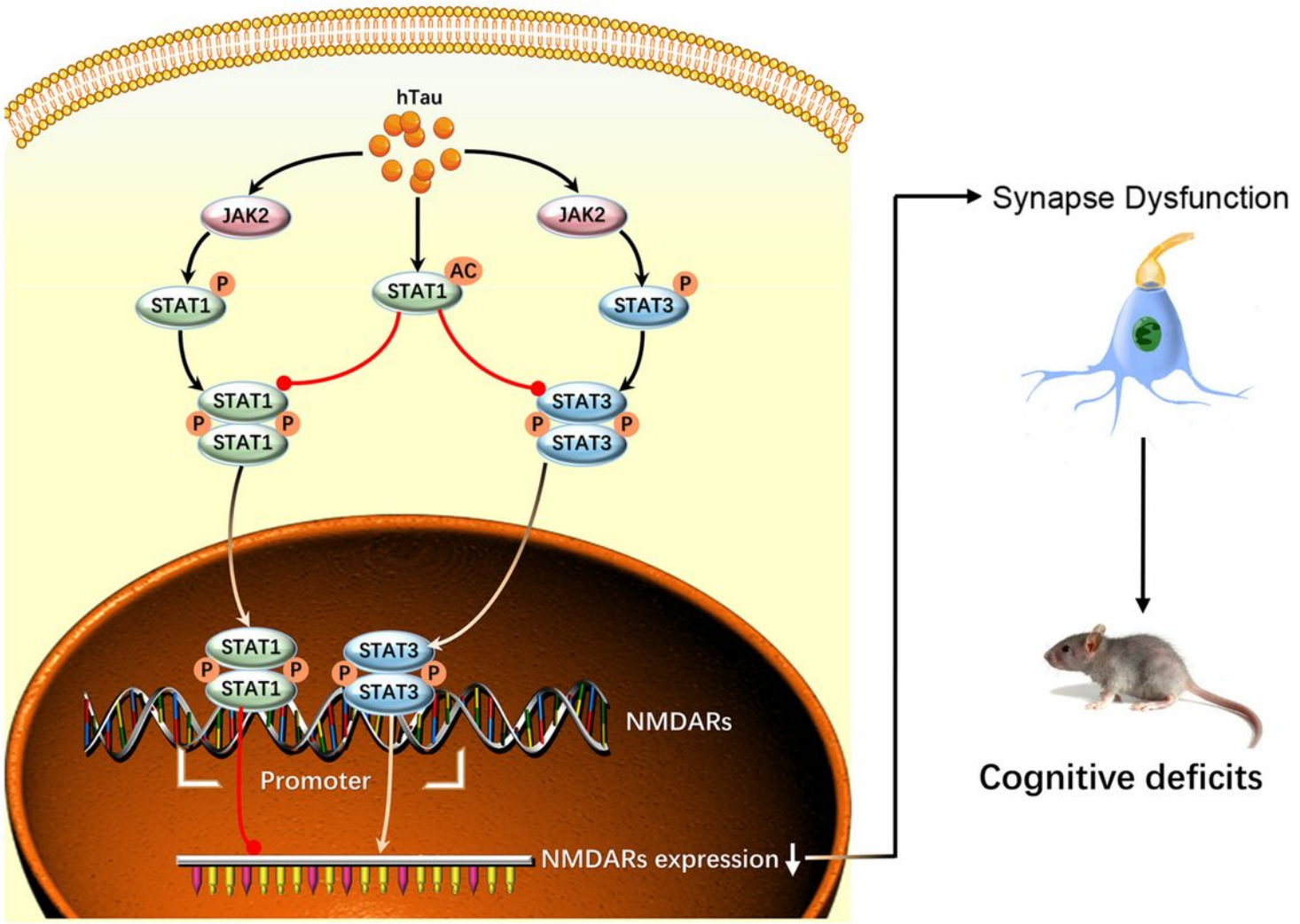

Figure 9

'Trade-off hypothesis' for hTau accumulation induced synaptic toxicities. Tau accumulation activated JAK2/STAT1 signaling pathway to phosphorylate STAT1 at Y701, promoted STAT1 to form a homodimer and translocate to the nucleus, thus activating STAT1 to suppress NMDARs expression and caused cognitive deficits. To rectify the adverse consequences of STAT1 activation, tau acetylated STAT1 to inhibit STAT1 nuclear translocation. However, acetylated STAT1 promoted STAT1 binding with STAT3 to

form a heterodimer in the cytoplasm and prevented STAT3 transport into the nucleus, though JAK2 also phosphorylated STAT3 at Y705. STAT1 negatively while STAT3 positively regulated NMDAR expression by binding to the specific GAS elements. Tau accumulation inhibited expression of NMDARs through upregulation of STAT1 activity and downregulation of STAT3 activity, ultimately leading to synaptic impairments and cognitive deficits.

Supplementary Files

This is a list of supplementary files associated with this preprint. Click to download.

- SupplementaryMaterials20190317230040.pdf